

Options and uncertainties in planetary defense: Mission planning and vehicle design for flexible response

Brent W. Barbee^{a,*}, Megan Bruck Syal^b, David Dearborn^b, Galen Gisler^c, Kevin Greenaugh^d, Kirsten M. Howley^b, Ron Leung^a, Josh Lyzloft^a, Paul L. Miller^b, Joseph A. Nuth^a, Catherine Plesko^c, Bernard D. Seery^a, Joseph Wasem^b, Robert P. Weaver^c, Melak Zebenay^a

^a NASA/Goddard Space Flight Center, 8800 Greenbelt Road, Greenbelt, MD, 20771, USA

^b Lawrence Livermore National Laboratory, 7000 East Avenue, P.O. Box 808, Livermore, CA, 94550, USA

^c Los Alamos National Laboratory, MST087, P.O. Box 1663, Los Alamos, NM, 87545, USA

^d National Nuclear Security Administration, Dept. of Energy, Forrestal Building, 1000 Independence Ave. SW, Washington, DC, 20585, USA

ABSTRACT

This paper is part of an integrated study by NASA and the NNSA to quantitatively understand the response timeframe should a threatening Earth-impacting near-Earth object (NEO) be identified. The two realistic responses considered are the use of a spacecraft functioning as either a kinetic impactor or a nuclear explosive carrier to deflect the approaching NEO. The choice depends on the NEO size and mass, the available response time prior to Earth impact, and the various uncertainties. Whenever practical, the kinetic impactor is the preferred approach, but various factors, such as large uncertainties or short available response time, reduce the kinetic impactor's suitability and, ultimately, eliminate its sufficiency.

Herein we examine response time and the activities that occur between the time when an NEO is recognized as being a sufficient threat to require a deflection and the time when the deflection impulse is applied to the NEO. To use a kinetic impactor for successful deflection of an NEO, it is essential to minimize the reaction time and maximize the time available for the impulse delivered to the NEO by the kinetic impactor to integrate forward in time to the eventual deflection of the NEO away from Earth impact.

To shorten the response time, we develop tools to survey the profile of needed spacecraft launches and the possible mission payloads. We further present a vehicle design capable of either serving as a kinetic impactor, or, if the need arises, serving as a system to transport a nuclear explosive to the NEO. These results are generated by analyzing a specific case study in which the simulated Earth-impacting NEO is modeled very closely after the real NEO known as 101955 Bennu (1999 RQ₃₆). Bennu was selected for our case study in part because it is the best-studied of the known NEOs. It is also the destination of NASA's OSIRIS-REx sample return mission, which is, at the time of this writing, enroute to Bennu following a September 2016 launch.

1. Introduction

For its report to the United States Congress, the 2010 National Research Council examined a broad range of NEO mitigation options [8]. It found that kinetic impactors could deflect most NEO threats discovered sufficiently far in advance, and that, when sufficient, kinetic impactors are the preferred option, in part because of their comparative simplicity and relative technological maturity. They are likely a relatively dependable and simple method for deflecting the more common, smaller asteroids, although no kinetic impactor has ever actually been demonstrated in space. NASA's 2005 Deep Impact mission succeeded in striking the ~5 km nucleus of comet 9P/Tempel 1, but the vast majority of NEO threats are much smaller and harder to hit; additionally, Deep Impact was not intended to make a measurable change in the comet's orbit and, as

such, no measurable change in the comet's orbit was made.

Time is needed for the initial impulse to integrate to a successful deflection, and the larger the asteroid, the more time is required. For scenarios in which warning time is limited such that the deflection impulse cannot be applied until several years or even several months before Earth impact, the necessary impulse magnitude for deflection will often become so large that is of the same order as the asteroid's surface escape velocity. In those situations, it is very likely that the required impulse for deflection would disrupt the asteroid, even though disruption is not the intention. In that situation a debris field would be created, regardless of the means by which the impulse is generated. Hence, delay and uncertainty significantly diminish the practicality of a kinetic impactor mission. If the NEO threat is from a large, more catastrophic NEO (which are, fortunately, less common than smaller NEOs), or the time to impact

* Corresponding author.

E-mail address: brent.w.barbee@nasa.gov (B.W. Barbee).

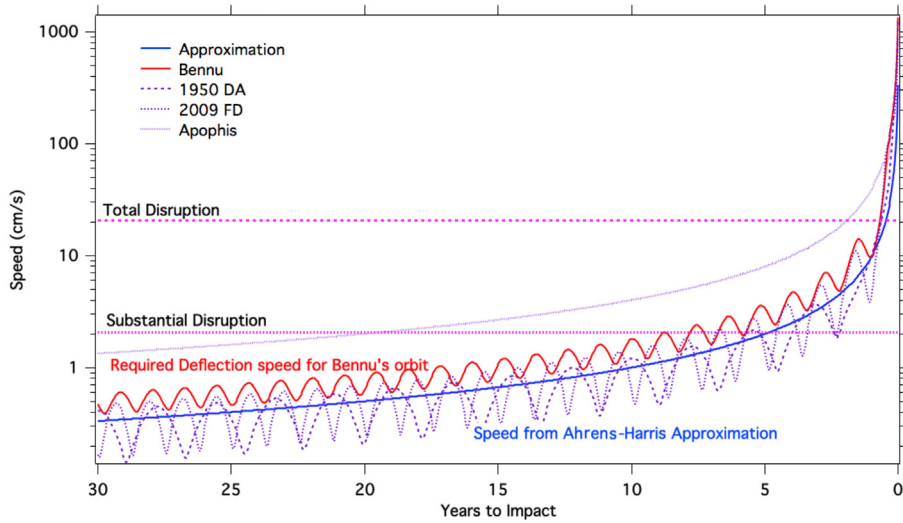


Fig. 1. Required deflection Δv (“speed”) versus time for a Bennu-like orbit.

is too short for a kinetic impactor mission to deflect the NEO without inadvertently weakly disrupting it, then robust disruption of the asteroid via nuclear device becomes the last alternative to simply allowing the asteroid to impact the Earth and conducting civil defense (disaster management on the ground). Note that even if a kinetic impactor is technically sufficient to disrupt an NEO, the disruption will be weak. That creates too great a chance of the remaining NEO fragments (a) being large enough to survive passage through our atmosphere, and (b) not being strongly dispersed, leaving a significant number of fragments on Earth-impacting trajectories. Nuclear devices are sufficiently energetic to break an NEO up into many very small and widely dispersed fragments that no longer pose a threat to Earth. We refer to that as robust disruption/dispersal.

NASA/NNSA have joined in an interagency agreement with several goals, including to study possible approaches to mitigating the threat posed by NEO collisions with Earth, to evaluate how the associated uncertainties influence the available mitigation options, and to assess which mitigation approaches are most likely to be most effective and which uncertainties have the most influence on outcomes. NASA brings expertise in planetary science, astrodynamics, and spacecraft mission design, while the NNSA brings expertise in computational modeling of energetic systems, such as kinetic impactors and nuclear devices, and laboratory experiments. The NNSA also has unique knowledge for evaluating nuclear systems. Together, NASA/NNSA have undertaken an integrated study of the steps required for an NEO mitigation mission.

NEO orbits around the Sun commonly have significant eccentricities and inclinations, limiting the available opportunities to launch massive payloads to such NEOs, especially for the high-speed approaches favorable to kinetic impactor performance. This work develops the methodology to examine the trade between payload mass, impact speed, launch opportunity frequency, and launch vehicle. An important parameter for mission planning is C_3 , a measure of the extra energy a launch vehicle can give a payload beyond that needed to barely escape the Earth-Moon system. Larger C_3 values enable more launch opportunities with higher impact speeds, but reduce payloads. Because the deflection enhancement of an impactor is sensitive to the achievable impact speed, the value of a higher-speed impact is multiplied, in general. That said, it should be noted that the achieved deflection also depends on the physical properties of the asteroid.

The NEO 101955 Bennu (1999 RQ₃₆) was selected for our first of three case studies (referred to as Case Study 1), and it provides a focus for the payload/launch opportunities study. Because it regularly passes close enough for radar observations (approximately every 6 years) sufficient measurement data exists to estimate its orbit with enough accuracy to achieve 100% certainty of an impact at least several years, and as much as a few decades, before the Earth collision event. NEOs for which radar observations are not available may reach an impact probability of 60 to 80% after telescopic observations (providing angle data, but no direct range measurements) span several Earth/NEO synodic periods, while 100% certainty of Earth collision may not be reached until less than a year before the Earth collision event.

Finally, we present an overview of the HAMMER (Hypervelocity Asteroid Mitigation Mission for Emergency Response) spacecraft design. It is a modular design capable of functioning either as a kinetic impactor for NEO deflection or as a nuclear device carrier for NEO deflection or disruption. It is designed to have a mass of ~ 8 metric tons, as mass is often important for kinetic impactor performance. The Delta IV Heavy launch vehicle is capable of launching an ~ 8 metric ton spacecraft to a relatively energetic Earth departure trajectory, and so the Delta IV Heavy serves as an example of a launch vehicle that would, in general, be sufficiently capable to launch the HAMMER on a range of NEO intercept missions.

Note that despite its relatively low bulk density, Bennu is very large (massive) for deflection by a kinetic impactor, and this was understood prior to the undertaking of our work. However, we felt it important to generate a detailed and quantitative assessment of how much kinetic impactor mass would be required (before including contingencies and redundancies to bolster mission success probability) to successfully deflect a Bennu-class NEO. These results raise important issues associated

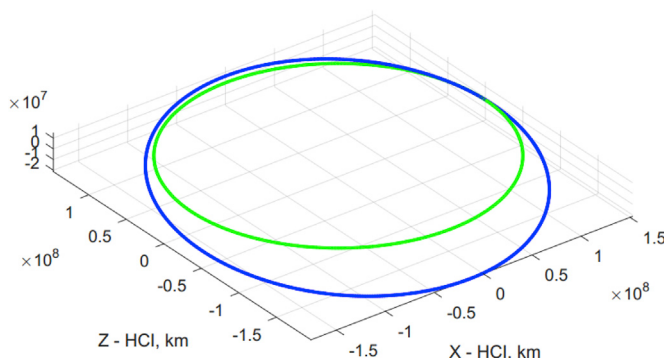


Fig. 2. The heliocentric orbits of Earth (green) and Bennu (blue), three-dimensional view. (For interpretation of the references to colour in this figure legend, the reader is referred to the web version of this article.)

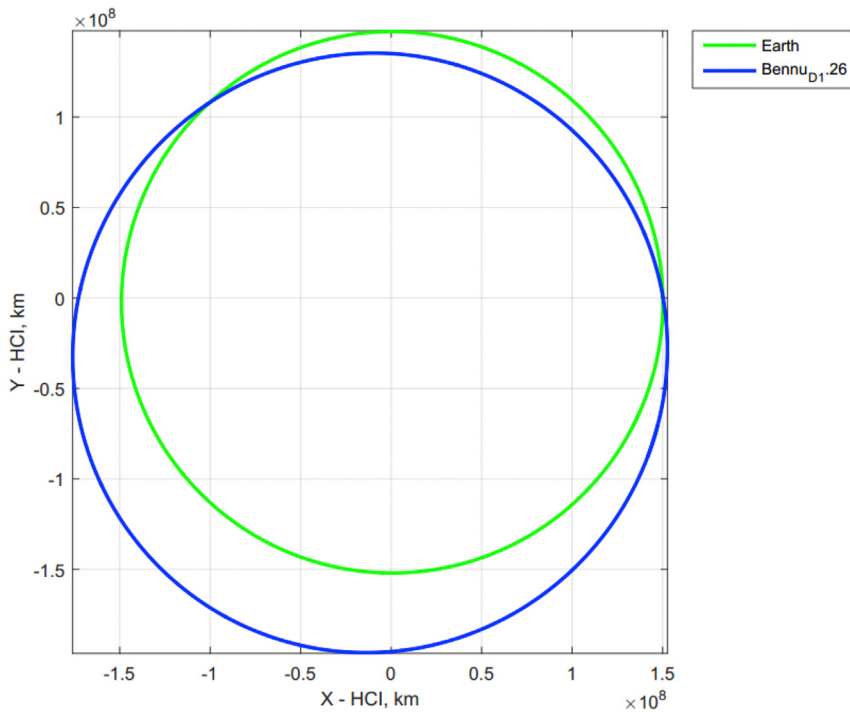


Fig. 3. The heliocentric orbits of Earth (green) and Bennu (blue), ecliptic plane projection. (For interpretation of the references to colour in this figure legend, the reader is referred to the web version of this article.)

with attempting multiple launches within a relatively short timeframe. Raising and assessing those issues is crucial if kinetic impactors are to be relied upon as a first-line defense against Earth-impacting NEOs. Impacts by NEOs as large as Bennu are, fortunately, thought to be very rare but could, in principle, happen at any time. Thus, it is very important to understand the limitations of kinetic impactor performance capabilities in such scenarios, so that we can be well informed and properly prepared to deal with large NEOs should the need arise. While the probability of facing such scenarios is low, the consequences of failing to be well enough prepared to respond successfully are so high as to be catastrophic. We also apply scaling techniques to our results for Bennu to assess for what size asteroids our kinetic impactor design would be practical for preventing Earth collision. In our second and third case studies, in

progress now and to be presented in future publications, we consider smaller NEOs that may be more tractable via kinetic impactors.

2. Overview of NEO 101955 Bennu (1999 RQ₃₆)

Bennu is a well-studied roughly spherical body (492 ± 20 m) with a total mass of $7.9 \pm 0.9 \times 10^{10}$ kg [2], and as the target of the OSIRIS-REx sample return mission [5] will provide a test of what we think we can learn about an asteroid from only remote (Earth-based) observations (by comparing the OSIRIS-REx spacecraft *in situ* measurements of Bennu to remote telescopic and radar measurements collected prior to the spacecraft visit). It is listed in the JPL Sentry System Risk Table as one of the objects most likely to impact the Earth in the future,

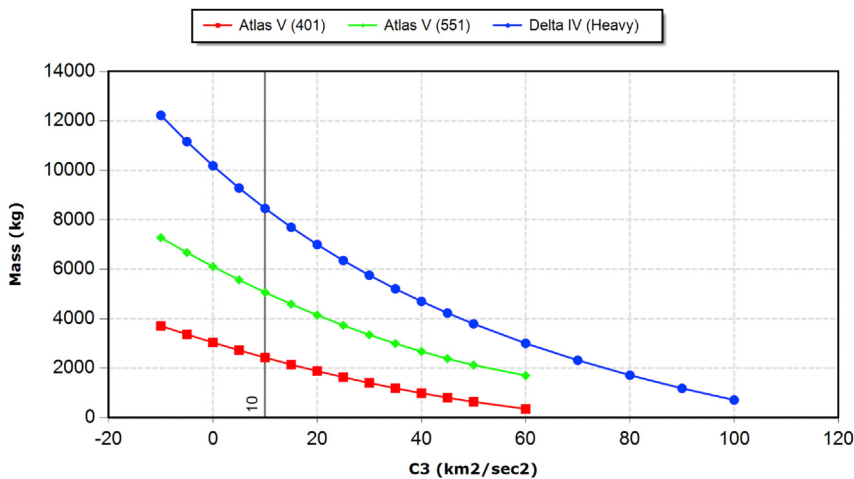


Fig. 4. Launch performance data for the Atlas V 401, Atlas V 551, and Delta IV Heavy launch vehicles.

Table 1

Constraints for Bennu deflection mission analysis.

	10 yr Launch Lead Time	25 yr Launch Lead Times
Minimum Distance From The Sun (AU)	0.7	0.7
Maximum Distance From The Sun (AU)	2.0	2.0
Minimum Departure Date	9/25/2125	9/25/2110
Maximum Departure Date	9/25/2133	9/25/2120
Maximum Arrival Date	9/15/2135	9/15/2135
Maximum Flight Time (days)	1500	1500
Minimum Declination of Launch Asymptote (DLA) (deg)	−28.5	−28.5
Maximum Declination of Launch Asymptote (DLA) (deg)	28.5	28.5
Maximum Phase Angle at Intercept (deg)	90	90
Minimum Sun-Spacecraft-Earth Angle at Intercept (deg)	3	3
Maximum C3 Value (km ² /s ²)	∞ (LV limited)	∞ (LV limited)

though the cumulative impact probability is still small: 3.7×10^{-4} (1 chance in 2700)¹. While there is no immediate concern, impact energy of a collision with Bennu is ~ 1.15 Gigatons, suggesting it as an interesting case study. The most threatening close approaches are predicted to occur late in the 22nd century.

Bennu's heliocentric orbit is relatively Earth-like, with an orbit semi-major axis near that of Earth's orbit, 1.12 au, a modest eccentricity, 0.2, and inclination of $\sim 6^\circ$. The difference in heliocentric speed between Bennu and the Earth during a time of close approach is relatively low (6.34 km/s), with a large gravitational impact parameter (2.8 Earth radii). The orbits of Earth and Bennu currently do not intersect, but the minimum orbit intersection distance (MOID) between their orbits is only 0.0032228 au, a bit more than a lunar distance (or 75 Earth radii), and is decreasing over time due to natural orbital perturbations.

Such orbits provide frequent launch opportunities, but most result in relative speeds at Bennu intercept that are low—generally non-optimal for deflection via kinetic impactors. In the case of Bennu, intercept trajectories from Earth that reach Bennu at 5 to 6 km/s relative speed are common. As will be examined later in this paper, there are also less frequent launch opportunities for trajectories that reach Bennu with relative speeds between 11 and 12 km/s (approximately every 6 years).

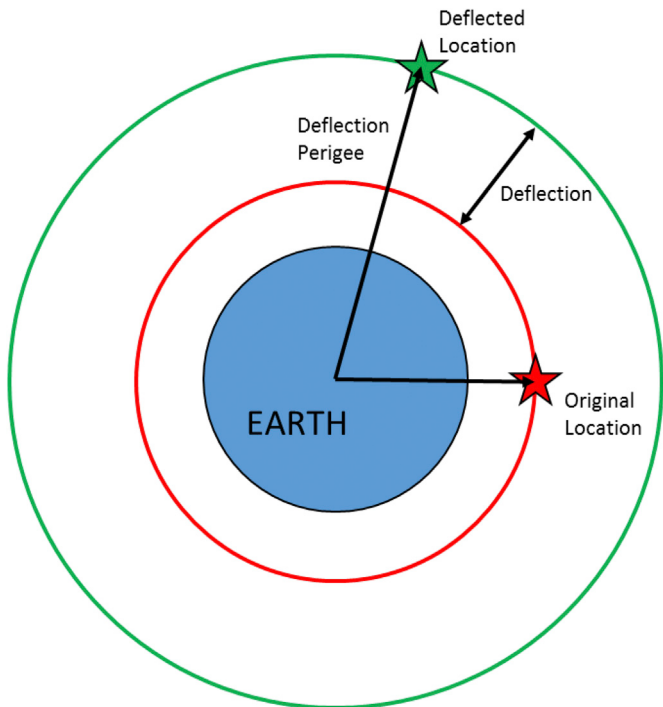
A final note on Bennu is that the large gravitational impact parameter, combined with the relatively low angle between Earth's and Bennu's orbits, increases the amount by which Bennu's velocity must be changed to avoid Earth collision beyond the usual approximation [1,6]:

$$\Delta v = \frac{10 \text{ cm/s}}{t \text{ (years)}} \quad (1)$$

Here Δv is the required change in the NEO's heliocentric inertial velocity required to deflect it away from Earth impact, and t is the time elapsed between when the deflection Δv is applied to the NEO and the unmitigated NEO/Earth collision date. This approximation is shown as a blue line in Fig. 1, where it can be compared to a more accurate result for an object with a Bennu-like orbit (red line). The more accurate result shows the well-known aphelion/perihelion periodic variation, in which the required Δv is minimized at perihelion. Note that the more accurate result requires up to nearly a factor of two more Δv for successful deflection than predicted by the approximation in Eq. (1).

3. Asteroid deflection astrodynamics and mission design

Thorough treatment of the problem of in-space mitigation of asteroids and comets requires consideration of several different types of missions

**Fig. 5.** Deflection definition illustration.

arranged within a mission campaign, the features of which are driven by the scenario parameters. For example, as discussed above, when the time available to act is very short, disruption of the asteroid may be the only practical option. Additionally, there may not be enough time to send a spacecraft to reconnoiter the asteroid in advance of the disruption mission, or to send a spacecraft to observe the effects of the disruption attempt. On the other hand, when more time is available to act, deflecting the asteroid (rather than disrupting it) becomes a viable option, and there may be opportunities to deploy an observer spacecraft to either fly by or rendezvous with the asteroid providing information about the asteroid's characteristics in advance of the deflection (or disruption) attempt, as well as continued observations for situational awareness during and after the mitigation attempt. Finally, a thorough treatment of the problem would involve including analyses specific to comets.

In the case study presented in this paper, we discuss only trajectory analysis for the interception of Bennu, with the goal of deflecting Bennu's heliocentric orbit via kinetic impact. However, the principles that apply to this analysis also apply to the broader problem set described above. Specific applications involving reconnaissance spacecraft, rendezvous versus intercept, mission campaign design, applicability to comet-like objects/orbits, and other related factors will be explored in our subsequent case studies.

Fig. 2 depicts the orbits of Bennu and Earth in three dimensions, while Fig. 3 displays the orbits projected onto the ecliptic plane (Earth's mean orbit plane). As discussed previously, Bennu's orbit is relatively Earth-like, giving rise to a range of opportunities to intercept the asteroid or rendezvous with it.

We seek to identify the sets of trajectories for kinetic impactor missions to Bennu that will deflect its subsequent motion by an amount sufficient to miss the Earth. To facilitate this analysis, we begin with the current definitive ephemeris for Bennu's orbit, obtained from JPL's Horizons system.² Bennu makes a very close approach to the Earth on September 25th, 2135, and we modify Bennu's ephemeris in our

¹ <https://cneos.jpl.nasa.gov/sentry/details.html?des=101955>, accessed on 2017-08-13.

² <http://ssd.jpl.nasa.gov/?horizons>, accessed on 2017-08-13.

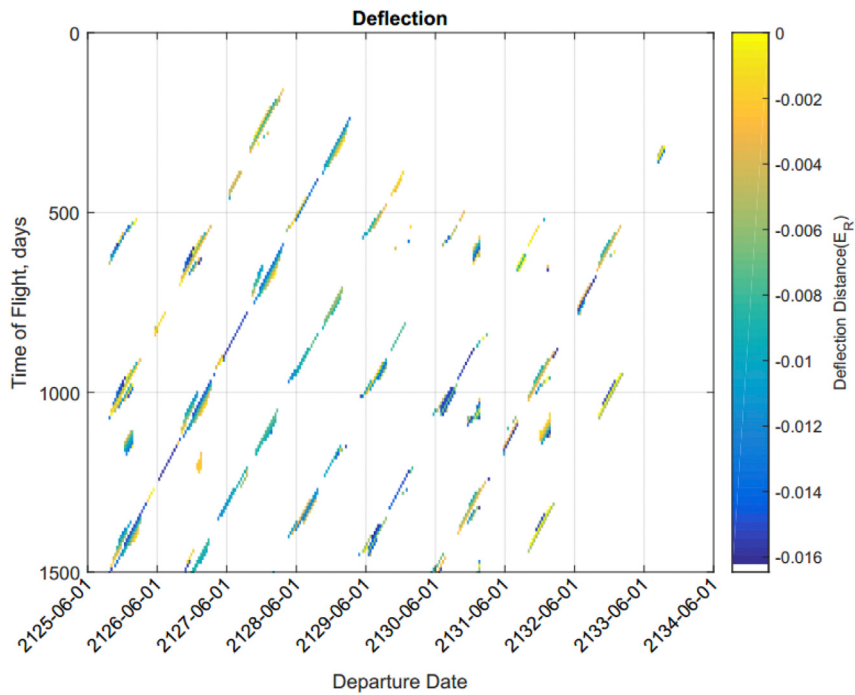


Fig. 6. Deflection solution space for the case of 1 HAMMER spacecraft launched on a Delta IV Heavy with a 10-year launch lead-time.

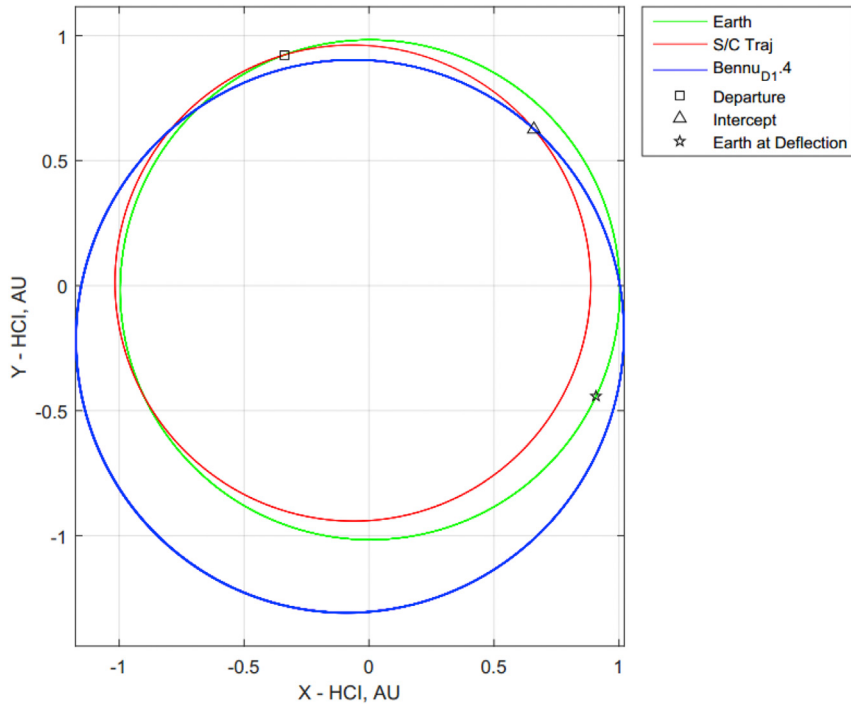


Fig. 7. Optimal deflection solution trajectory for the case of 1 HAMMER spacecraft launched on a Delta IV Heavy with a 10-year launch lead-time (ecliptic plane projection).

dynamics model slightly such that it instead hits the center of the Earth on that date. This provides our baseline Bennu orbit, against which our deflection calculations are performed. The objective of the trajectory optimization analysis is to maximize the minimum distance of Bennu from the Earth's surface (i.e., perigee altitude) during the September 2135 encounter, subject to various constraints.

In this analysis we model realistic launch vehicle performance. The launch vehicle performance is expressed in terms of the amount of mass

(kg) that the launch vehicle can inject into an outbound hyperbola that departs the Earth-Moon system with a particular value of specific energy, denoted as C_3 (km^2/s^2). These data are obtained from NASA Launch Services Program's Launch Vehicle Performance Website,³ and example data from that website for several common launch vehicles are

³ <https://elvperf.ksc.nasa.gov/Pages/Default.aspx>, accessed on 2017-08-13.

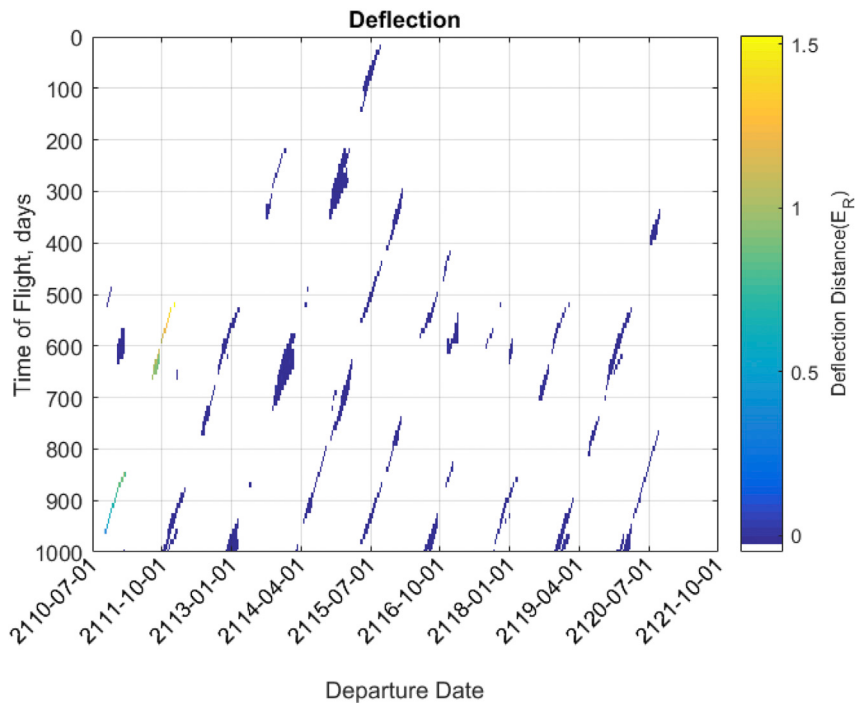


Fig. 8. Deflection solution space for the case of 17 HAMMER spacecraft launched on Delta IV Heavy launch vehicles with a 25-year launch lead-time.

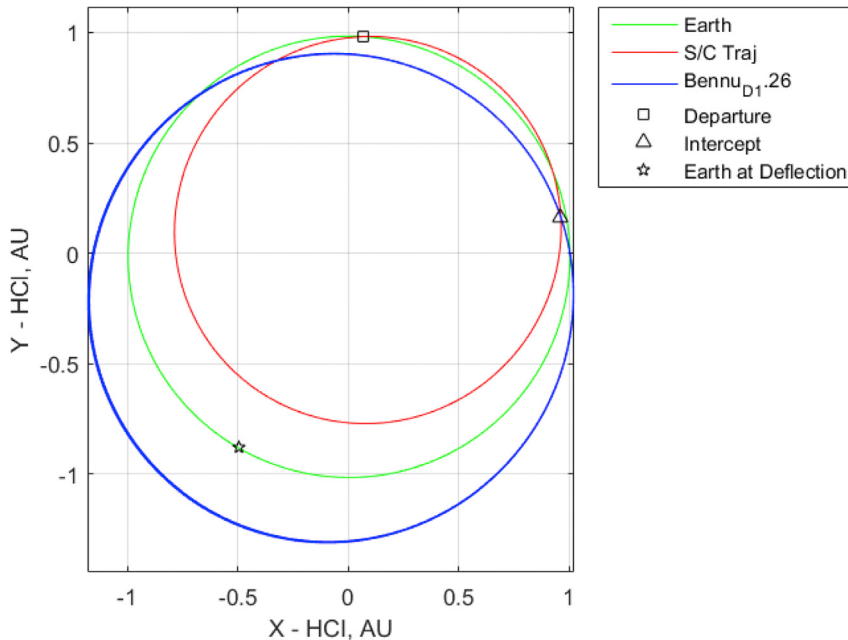


Fig. 9. Optimal deflection solution trajectory for the case of 17 HAMMER spacecraft launched on a Delta IV Heavy launch vehicles with a 25-year launch lead-time (ecliptic plane projection).

shown in Fig. 4.

Of the launch vehicles shown in Fig. 4, only the Delta IV Heavy offers sufficient performance to be of interest for kinetic impact deflection of an asteroid as large as Bennu. The smaller, less expensive Atlas V launch vehicles are shown only for comparison. We also model the estimated performance of NASA's proposed heavy-lift Space Launch System (SLS) launch vehicle, the estimated launch performance curves for which are

not yet publicly available.⁴ In general terms, the estimated performance of the Block 1 SLS with iCPS is approximately twice the performance of the Delta IV Heavy.

⁴ Note, however, that the estimated performance of the largest SLS design variant, the Block 2B, can be derived from data points on the publicly available NASA/JPL NEO Deflection App website, <https://cneos.jpl.nasa.gov/nda/>, accessed on 2017-08-13.

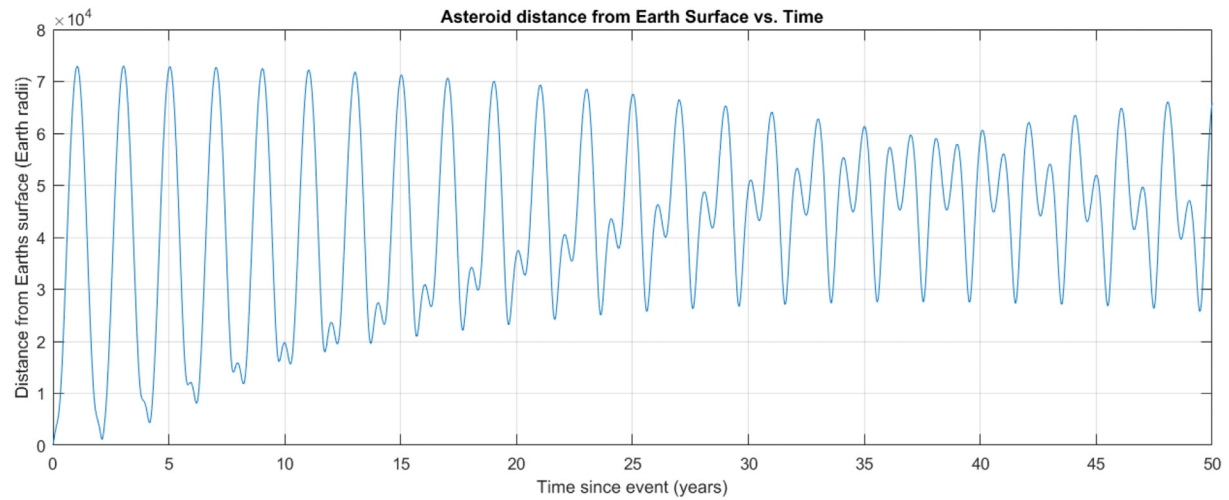


Fig. 10. Distance between Bennu and Earth, in units of Earth radii, for 50 years following the Earth close approach after the optimal deflection solution for the case of 17 HAMMER spacecraft launched on a Delta IV Heavy launch vehicles with a 25-year launch lead-time.

We incorporate the launch vehicle performance by first constructing a curve fit to the published data, as shown in Fig. 4, which allows us to quickly calculate the amount of mass that the launch vehicle can place onto an Earth departure trajectory of a given C_3 energy. Then, for every Earth-to-Bennu trajectory computed by our algorithms, we calculate the required Earth departure C_3 value and use the aforementioned launch vehicle performance curve fit equation to compute how much spacecraft mass the launch vehicle can place onto that particular Earth-to-Bennu trajectory. In some cases we allow all of that spacecraft mass to be collide with Bennu, while in other cases we restrict the mass to be quantized in terms of number of HAMMER spacecraft. Further discussion of launch vehicle selection for planetary defense missions may be found in Refs. [16] and [17].

The parameters for our model of Bennu for purposes of computing kinetic impactor effects on the asteroid are:

- Asteroid diameter of 500 m (spherical shape)

- Asteroid bulk density of 1.26 g/cm^3
- Momentum enhancement factor, β , of 1, except where otherwise noted below
- Precise definitive asteroid orbit ephemeris from JPL Horizons, modified to hit the center of the Earth on September 25, 2135

From the assumed spherical shape model and density, the derived mass of Bennu in our model is $8.24668 \times 10^{10} \text{ kg}$. This is at the upper end of the Bennu mass range mentioned previously [2].

We consider two situations in this analysis: a 10-year launch lead-time, and a 25-year launch lead-time. In our parlance, a 10-year launch lead-time means that trajectories are allowed to depart Earth no more than 10 years in advance of the Bennu/Earth collision date, and a 25-year launch lead-time means that trajectories are allowed to depart Earth no more than 25 years in advance of the Bennu/Earth collision date. The resulting constraints on Earth departure date, along with the other mission design constraints enforced in our analysis, are summarized in Table 1. Note that launch lead-time is not the same as warning time, because some amount of time will elapse between when the threatening asteroid is discovered and when we would be ready to launch a spacecraft to the asteroid. Thus, a 10-year launch lead-time means that more than 10 years of warning would have been required, for example.

Note that the spacecraft is not allowed to pass closer than 0.7 au (Venus orbit distance) to the Sun, because of possible thermal and radiation problems. Additionally, the spacecraft is not allowed to travel farther away from the Sun than 2.0 au, to avoid possible solar array power issues. These constraints are notional and considered representative, but would vary according to the particulars of a given spacecraft design. Therefore, the constraints should not be considered absolute, e.g., a spacecraft with an appropriate design could pass closer to the Sun than 0.7 au, or further from the Sun than 2.0 au.

The maximum time of flight (Earth to Bennu) is constrained to 1500 days, simply because experimentation with longer flight time values did not demonstrate appreciable benefit. The constraints on the Declination of the Launch Asymptote (DLA) of $\pm 28.5^\circ$ correspond to launch from Cape Canaveral Air Force Station (CCAFS) at NASA's Kennedy Space Center (KSC) in Florida. Launching a spacecraft to DLA values outside of the specified bounds violates the assumptions behind the launch vehicle performance curves discussed previously, and would require special negotiation with the launch services provider. In cases where the DLA is far outside the stated bounds, launch from CCAFS may not even be feasible, and a launch site at a different latitude would be required.

The maximum allowed solar phase angle at asteroid intercept is set to

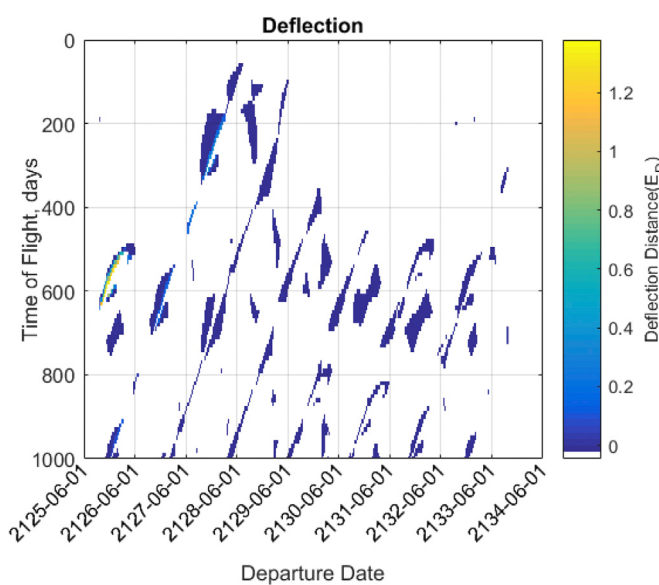


Fig. 11. Deflection solution space for the case of 29 SLS Block 1 w/iCPS launches, each using all available launch mass capacity, with a 10-year launch lead-time.

Table 2
Deflection of at least ~1.4 RE from Earth's surface and $\beta = 1$.

Available Launch Lead Time (yrs)	Launch Vehicle	Number of Launches	Return Impact within 50 Years	Used KI Mass (kg)	Total Specific Energy Imparted to NEO (J/kg)	Time from Defl. to Earth Encounter (yrs)	Δv Imparted to NEO (cm/s)	Defl. (R_e)	Defl. Perigee (R_e)	Defl. Bplane (R_e)	
10	Delta IV Heavy	1	N/A	9072.64	1.051512	1.15	0.045632	-0.168	0.832	0.085	
10	Delta IV Heavy (HAMMER)	1	N/A	7300	1.358724	1.07	0.046529	-0.169	0.831	0.065	
10	Delta IV Heavy (HAMMER)	1	N/A	7300	1.358724	1.07	0.046529	-0.169	0.831	0.065	
10	Adjusted Mass (max mass 7300)	SLS Block 1 w/ICPS	1	N/A	3085.54	0.750999	0.55	0.022490	-0.172	0.828	0.031
10	Delta IV Heavy	75	No	627090.90	258.23607	8.22	6.266800	1.432	2.432	3.786	
10	Delta IV Heavy (HAMMER)	83	No	605900.00	307.56012	8.24	6.722607	1.435	2.435	3.789	
10	Delta IV Heavy (HAMMER)	83	No	605900.00	307.56012	8.24	6.722607	1.435	2.435	3.789	
10	Adjusted Mass (max mass 7300)	SLS Block 1 w/ICPS	29	No	628520.77	258.82489	8.22	6.281089	1.440	2.440	3.794
25	Delta IV Heavy	1	N/A	8405.80	2.750032	22.37	0.074874	-0.202	0.798	0.234	
25	Delta IV Heavy (HAMMER)	1	N/A	7300	3.882061	22.34	0.082903	-0.213	0.787	0.244	
25	Delta IV Heavy (HAMMER)	1	N/A	7300	3.882061	22.34	0.082903	-0.213	0.787	0.244	
25	Adjusted Mass (max mass 7300)	SLS Block 1 w/ICPS	1	N/A	21811.95	7.135973	22.37	0.194289	-0.213	-0.787	0.607
25	Delta IV Heavy	16	No	134491.38	43.997952	22.37	1.197949	1.384	2.384	3.733	
25	Delta IV Heavy (HAMMER)	17	No	124100.00	65.995730	22.34	1.409349	1.444	2.444	3.799	
25	Delta IV Heavy (HAMMER)	17	No	124100.00	65.995730	22.34	1.409349	1.444	2.444	3.799	
25	Adjusted Mass (max mass 7300)	SLS Block 1 w/ICPS	6	No	130870.07	42.813265	22.37	1.165693	1.294	2.294	3.632

90°, representing the asteroid being at least half lit by the sun from the spacecraft's perspective during terminal approach to intercept. This is intended as a notional, representative constraint that assumes the spacecraft's terminal guidance sensor operates in the visible band. In practice, this constraint will vary according to the particular spacecraft and terminal guidance sensor design. For example, a terminal guidance sensor operating at infrared wavelengths may not have issues with higher phase angles.

The minimum allowed sun-spacecraft-Earth angle at asteroid intercept is set to 3°, because for geometries corresponding to smaller values of this angle, the Deep Space Network (DSN) cannot guarantee a radio link with the spacecraft due to solar interference. Here we assume that communications with the spacecraft will be required during the critical mission event of asteroid intercept.

Removing the constraints on minimum/maximum distance to the Sun resulted in only marginal improvements to asteroid deflection performance, and those marginally improved deflection solutions involve closest approach to the Sun of 0.4–0.6 au. Thus, designing the interceptor spacecraft to be able safely pass closer than 0.7 au to the Sun would be relevant to deflection of Bennu. On the other hand, removing or relaxing the other constraints (e.g., DLA, approach phase angle, SSE angle, etc) did not lead to notable deflection performance improvements. However, relaxing those constraints does yield some increase in the number of viable mission launch opportunities. Note that those constraint sensitivities are particular to Bennu's orbit and the situation will generally vary with NEO orbit.

Our algorithms utilize a grid search to identify all sets of feasible asteroid deflection trajectory solutions (i.e., solutions that deflect the asteroid away from Earth by at least some given distance), and then identify the optimal (maximal deflection) solution from within the sets of feasible solutions. The Earth-to-Bennu trajectories are computed using a multi-revolution Lambert solver⁵ [3,4,7] applied to precise Earth ephemeris (obtained from the JPL Horizons system) and the aforementioned customized Bennu ephemeris. The deflected asteroid trajectories are propagated using the “ode113” numerical integrator in MATLAB, operating on an N-body solar system dynamics model that includes the gravity of the Moon, Mercury, Venus, Mars Barycenter, Earth (including the J_2 non-spherical gravity effects), Jupiter Barycenter, Saturn Barycenter, Uranus Barycenter, Neptune Barycenter, and Pluto Barycenter. However, 10 days prior to Earth closest approach, the propagation of the asteroid's motion switches to a Lie Group Variational Integrator (LGVI) to better identify the exact epoch of closest approach via a discrete Equations of Motion (EOM) formulation and a 1/1000th of a day time step.

The Δv vector imparted to the asteroid by the spacecraft impact is computed according to the conservation of linear momentum, given by:

$$\Delta \vec{v} = \beta \frac{m}{m+M} (\vec{v}_{sc} - \vec{v}_a) \quad (2)$$

where β is the momentum enhancement factor that scales the magnitude of the imparted $\Delta \vec{v}$ vector according to how much impact ejecta contributes to the momentum transferred to the asteroid, m is the mass of the spacecraft, M is the mass of the asteroid, the \vec{v}_{sc} vector is the heliocentric inertial velocity of the spacecraft at the time of asteroid impact, and the \vec{v}_a vector is the heliocentric inertial velocity of the asteroid at the same epoch.

In the results that follow, we utilize the definitions of deflection depicted in Fig. 5. The original location of the asteroid at its closest approach to the Earth may be on the Earth's surface, if the original (i.e., undeflected) motion of the asteroid results in an Earth collision, as is the case for our modified Bennu ephemeris, as described previously.

Deflection is computed as the difference between (a) the distance of

⁵ Available online at <https://www.mathworks.com/matlabcentral/fileexchange/26348-robust-solver-for-lambert-s-orbital-boundary-value-problem?requestedDomain=www.mathworks.com>, accessed on 2017-08-13.

Table 3Deflection of at least ~ 0.25 RE from Earth's surface and $\beta = 1$.

Available Launch Lead Time (yrs)	Launch Vehicle	Number of Launches	Return Impact within 50 Years	Used KI Mass (kg)	Total Specific Energy Imparted to NEO (J/kg)	Time from Defl. to Earth Encounter (yrs)	Δv Imparted to NEO (cm/s)	Defl. (R_e)	Defl. Perigee (R_e)	Defl. Bplane (R_e)
10	Delta IV Heavy	1	N/A	9072.64	1.051512	1.15	0.045632	-0.168	0.832	0.085
10	Delta IV Heavy (HAMMER)	1	N/A	7300	1.358724	1.07	0.046529	-0.169	0.831	0.065
10	Delta IV Heavy (HAMMER)	1	N/A	7300	1.358724	1.07	0.046529	-0.169	0.831	0.065
Adjusted Mass (max mass 7300)										
10	SLS Block 1 w/iCPS	1	N/A	3085.54	0.750999	0.55	0.022490	-0.172	0.828	0.031
10	Delta IV Heavy	48	No	401338.2	165.271083	8.22	4.010763	0.248	1.248	2.422
10	Delta IV Heavy (HAMMER)	53	No	386900.0	196.392874	8.24	4.292750	0.246	1.246	2.418
10	Delta IV Heavy (HAMMER)	53	No	386900.0	196.392874	8.24	4.292750	0.246	1.246	2.418
Adjusted Mass (max mass 7300)										
10	SLS Block 1 w/iCPS	19	No	411789.5	169.574927	8.22	4.115207	0.300	1.300	2.485
25	Delta IV Heavy	1	N/A	8405.80	2.750032	22.37	0.074874	-0.202	0.798	0.234
25	Delta IV Heavy (HAMMER)	1	N/A	7300	3.882061	22.34	0.082903	-0.213	0.787	0.244
25	Delta IV Heavy (HAMMER)	1	N/A	7300	3.882061	22.34	0.082903	-0.213	0.787	0.244
Adjusted Mass (max mass 7300)										
25	SLS Block 1 w/iCPS	1	N/A	21811.95	7.135973	22.37	0.194289	-0.213	-0.787	0.607
25	Delta IV Heavy	10	No	92463.79	30.250348	22.37	0.823618	0.381	1.381	2.575
25	Delta IV Heavy (HAMMER)	11	No	80300.00	42.702672	22.34	0.911927	0.292	1.292	2.466
25	Delta IV Heavy (HAMMER)	11	No	80300.00	42.702672	22.34	0.911927	0.292	1.292	2.466
Adjusted Mass (max mass 7300)										
25	SLS Block 1 w/iCPS	4	No	87247.81	28.543894	22.37	0.777157	0.264	1.264	2.430

Table 4Deflection of at least ~ 1.4 RE from Earth's surface and $\beta = 2.5$.

Available Launch Lead Time (yrs)	Launch Vehicle	Number of Launches	Return Impact within 50 Years	Used KI Mass (kg)	Total Specific Energy Imparted to NEO (J/kg)	Time from Deflection to Earth Encounter (yrs)	Δv Imparted to NEO (cm/s)	Defl. (R_e)	Defl. Perigee (R_e)	Defl. Bplane (R_e)
10	Delta IV Heavy	1	N/A	9045.11	2.203519	4.71	0.16489	-0.165	0.835	0.139
10	Delta IV Heavy (HAMMER)	1	N/A	7300	1.223178	0.06	0.11037	-0.172	0.828	0.017
10	Delta IV Heavy (HAMMER)	1	N/A	7300	1.223178	0.06	0.11037	-0.172	0.828	0.017
Adjusted Mass (max mass 7300)										
10	SLS Block 1 w/iCPS	1	N/A	13507.25	9.752915	2.44	0.42392	-0.164	0.836	0.153
10	Delta IV Heavy	30	No	250836.36	103.2944	8.22	6.26683	1.432	2.432	3.786
10	Delta IV Heavy (HAMMER)	34	No	248200	125.9879	8.24	6.88461	1.519	2.519	3.880
10	Delta IV Heavy (HAMMER)	34	No	248200	125.9879	8.24	6.88461	1.519	2.519	3.880
Adjusted Mass (max mass 7300)										
10	SLS Block 1 w/iCPS	12	No	260077.56	107.1	8.22	6.49771	1.560	2.560	3.925
25	Delta IV Heavy	1	N/A	8405.8	2.750032	22.37	0.18719	-0.224	0.776	0.584
25	Delta IV Heavy (HAMMER)	1	N/A	7300	3.882061	22.34	0.20726	-0.221	0.779	0.560
25	Delta IV Heavy (HAMMER)	1	N/A	7300	3.882061	22.34	0.20726	-0.221	0.779	0.560
Adjusted Mass (max mass 7300)										
25	SLS Block 1 w/iCPS	1	N/A	21811.95	7.135973	22.37	0.48572	-0.191	0.809	1.517
25	Delta IV Heavy	7	No	58839.98	19.24910	22.37	1.31026	1.703	2.703	4.083
25	Delta IV Heavy (HAMMER)	7	No	51100.00	27.17471	22.34	1.45080	1.546	2.546	3.911
25	Delta IV Heavy (HAMMER)	7	No	51100.00	27.17471	22.34	1.45080	1.546	2.546	3.911
Adjusted Mass (max mass 7300)										
25	SLS Block 1 w/iCPS	3	No	65435.04	21.40663	22.37	1.45712	2.126	3.216	4.540

Table 5

Effects of Density and β on HAMMER performance, when deflection of at least 1.4 RE from Earth's surface is required.

Available Launch Lead Time (yrs)	β	Asteroid Density (g/cm^3)	Diameter (m)	Deflection (R_\oplus)	Specific Energy (J/kg)	Escape velocity fraction ($\frac{\Delta v}{v_{\text{esc}}}$)
10	1	1	123.8	1.436	307.587357	1.452552
10	1	2.6	90.03	1.436	307.606364	1.238811
10	2.5	1	168.02	1.436	123.040326	1.070316
10	2.5	2.6	122.19	1.436	123.041062	0.912753
25	1	1	210.028	1.444	65.995738	0.179480
25	1	2.6	152.74	1.456	65.995028	0.153056
25	2.5	1	285.052	1.456	26.397977	0.132241
25	2.5	2.6	207.300	1.456	26.398039	0.112773

the original location of closest approach from the center of the Earth and (b) the distance of the deflected trajectory's closest approach from the center of the Earth. We also compute the deflection perigee for a deflected asteroid trajectory, which is the closest approach distance from the Earth's surface for the asteroid on its deflected trajectory.

The nature of the deflection trajectory solution space is shown in Fig. 6, in which the achieved deflection is plotted for every combination of Earth departure date and Earth-to-Bennu flight time, subject to the aforementioned constraints. The particular data set displayed in Fig. 6 corresponds to the case in which a single HAMMER spacecraft is launched via Delta IV Heavy launch vehicle, with a 10-year lead-time. Note that this case is non-functional from an asteroid deflection perspective, as the spacecraft has a negligible effect on the asteroid's orbit, and most of the kinetic impact trajectories results in actually pushing the asteroid slightly closer to the center of the Earth. The trajectory solution corresponding to the optimal (maximal) deflection solution contained within Fig. 6 is shown in Fig. 7.

In addition to examining the capability of a single HAMMER spacecraft to deflect Bennu's orbit, we ran our algorithms in an investigative mode, to identify the minimum number of HAMMER spacecraft launches required to achieve a Bennu deflection of at least ~ 1.4 Earth radii. With a 25-year lead-time, 17 HAMMER spacecraft (launched via Delta IV Heavy launch vehicles) are required, and the resulting solution space is shown in Fig. 8.

The trajectory solution corresponding to the optimal (maximal) deflection solution contained within Fig. 8 is shown in Fig. 9. Our algorithm also propagates the post-deflection orbit of the asteroid past the Earth closest approach, to be sure that the asteroid does not encounter any gravitational keyholes during its close approach to the Earth on the deflected trajectory. Gravitational keyholes are regions in spacetime relative to the Earth, defined such that if the asteroid were to pass through a keyhole, Earth's gravity would alter the asteroid's heliocentric orbit in a way that would cause it to re-encounter (and collide with) the Earth some number of years later. Our software propagates each apparently viable asteroid deflection solution for 50 years after the first Earth close approach after deflection and then discards any deflection solutions that result in uncomfortably close Earth approaches by the asteroid within the 50-year propagation interval. As an example, the distance between Bennu and Earth after post-deflection Earth close approach is plotted in Fig. 10. While the asteroid does pass within several thousand Earth radii of the Earth several years after the initial Earth close approach, the asteroid's minimum distance to Earth increases to nearly

30,000 Earth radii over the next several decades.

Returning to the case of a 10-year launch lead-time, we find that 29 SLS Block 1 w/iCPS launch vehicles (using all of the available launch vehicle mass capability, i.e., not enforcing that the launch mass must be quantized into HAMMER spacecraft) are required to deflect Bennu by ~ 1.4 Earth radii with a 10-year launch lead-time. The corresponding deflection solution space is shown in Fig. 11.

In contrast to the previous case, it is of note that the asteroid does come within 332 Earth radii (~ 2.1 million km) of the Earth approximately 44 years after the post-deflection Earth encounter (at ~ 1.4 Earth radii).

The overall set of results for the various cases studies is summarized in Table 2. These results include both Delta IV Heavy and SLS Block 1 launch vehicle options, either 10-year or 25-year launch lead-time, single or multiple launch, and either quantization of available spacecraft launch mass into a number of discrete HAMMER spacecraft, or utilization of all available spacecraft launch mass capability without packaging that mass into individual HAMMER spacecraft.

The results in Table 2 show that, with an assumed β of 1, a maximum launch lead-time of 25 years, and a requirement to achieve a deflection of at least ~ 1.4 Earth radii, neither the Delta IV Heavy nor the SLS Block 1 is able to deflect Bennu with a single launch. Furthermore, the number of launches required is extremely large, ranging from 29 to 83 for the 10-year launch lead-time cases. Somewhat fewer launches are required for the 25-year launch lead-time cases, in which the required number of launches is approximately 17 for the Delta IV Heavy or 6 for the SLS Block 1. An additional concern is that the specific energy imparted to the asteroid is high (~ 250 – 300 J/kg) for the many-launch 10-year launch lead-time cases that achieve ~ 1.4 Earth radii deflection. For reference, it is possible that the asteroid could be undesirably disrupted at deflection specific energy levels of ~ 100 J/kg, although this is currently an area that requires further research.

Some discussion of the issues surrounding missions involving multiple launches is warranted here, in view of the fact that the various kinetic impactor mission solutions for deflecting Bennu require multiple launches. Contemporary spacecraft missions require but a single launch (for reasons of financial cost minimization and mission reliability maximization), making a mission that requires a coordinated set of multiple launches within a relatively short time frame rather unprecedented. Because of this, the necessary infrastructures for launch vehicle production and launch facility logistics are not currently available. As such, it would not currently be practical to execute a planetary defense mission

Table 6

Effects of Density and β on HAMMER performance, when deflection of at least 0.25 RE from Earth's surface is required.

Available Launch Lead Time (yrs)	β	Asteroid Density (g/cm^3)	Diameter (m)	Deflection (R_\oplus)	Specific Energy (J/kg)	Escape velocity fraction ($\frac{\Delta v}{v_{\text{esc}}}$)
10	1	1	143.62	0.252	197.008810	0.801965
10	1	2.6	104.4456	0.252	197.009251	0.683903
10	2.5	1	194.922	0.252	78.803923	0.590899
10	2.5	2.6	141.75	0.252	78.811186	0.503969
25	1	1	244.6	0.251	41.780494	0.097566
25	1	2.6	177.881	0.251	41.781198	0.083204
25	2.5	1	331.9733	0.249	16.712194	0.071887
25	2.5	2.6	241.123	0.256	16.774658	0.061610

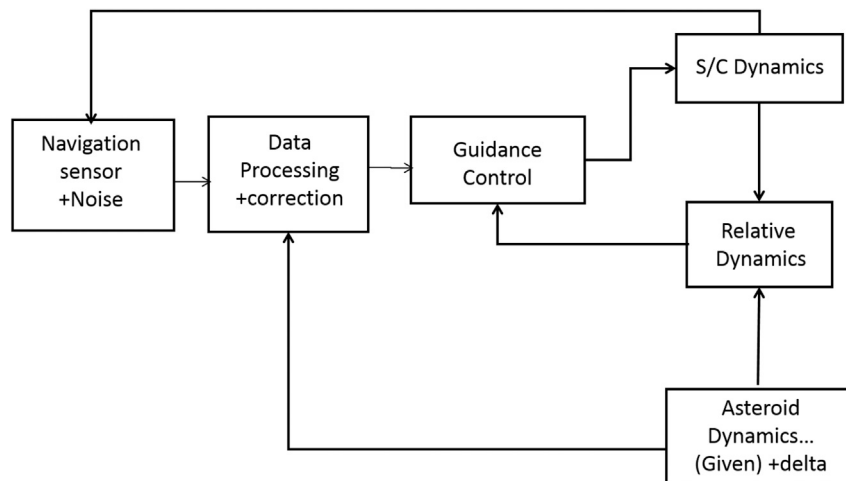


Fig. 12. Block diagram of NEO Intercept GNC concept.

that requires multiple launches in a relatively short time frame (e.g., over the course of several weeks to several months). Assuming all of the needed launch vehicles could be constructed in the necessary timeframe without loss of operational reliability, some minimum amount of time will be required by the various launch facilities to refresh their launch pads in between individual launches, and that minimum amount of time between launches is not currently known. Further analysis in cooperation with various launch vehicle manufacturers and launch services providers would be required to begin understanding actual capabilities for conducting missions requiring multiple coordinated launches within a relatively short time frame. Those analyses should be followed up by emergency drill exercises and even representative test flights, to prove that the results of the analyses are valid. Additionally, research to quantify the impacts of multiple launches on overall mission reliability are required. All of those issues are beyond the scope of the work presented here, but the aforementioned issues should be kept in mind when assessing the mission design results shown herein.

Note that the deflection perigee values achieved for the successful cases in Table 2 are on the order of ~2.3–2.5 Earth radii. It may be that a minimally successful asteroid deflection only requires a deflection perigee altitude on the order of ~0.25 Earth radii (to essentially just barely miss the Earth), corresponding to a deflection perigee radius of ~1.25 Earth radii. Thus, the results in Table 2 may be considered to be

minimally robust, while a ~0.25 Earth radii deflection perigee results set could be considered minimally functional. To understand the reduction in launch costs associated with relaxing the deflection requirement to a deflection perigee of ~0.25 Earth radii, the study was repeated with that setting, and the results are summarized in Table 3.

Note that only requiring a ~1.25 Earth radii deflection perigee radius results in only requiring deflection values on the order of ~0.3 Earth radii, much smaller than the ~1.4 Earth radii deflection required in the first results set. The number of launches required for the 10-year launch lead-time cases is still extremely high, ranging from 19 to 53 launches. The number of launches required in the 25-year cases are also proportionately reduced, but still formidable at 11 Delta IV Heavy launches or 4 SLS Block 1 launches.

We next consider the effects of β on the results. As noted previously, β will linearly scale the magnitude of the ΔV vector imparted to the asteroid by the kinetic impactor(s). We return to the case of requiring a deflection of ~1.4 Earth radii (which we may, perhaps, consider minimally robust) and reassess performance with a β of 2.5 (rather than the original value of $\beta = 1$). The results are presented in Table 4.

Note that changing from $\beta = 1$ to $\beta = 2.5$ has a nearly linear (inverse) effect on the required number of launch vehicles, modulated by the fact that we model an integer number of launches (i.e., we cannot, of course, have fractional launches). This is a significant effect, and so we are motivated to seek an improved understanding of β , work that will be reported on in Paper 1. That said, even with $\beta > 1$ we would need to deploy tens of metric tons worth of mass in order to just barely deflect Bennu (or an asteroid of similar size/mass on a similar orbit to Bennu's).

From the foregoing results we find a HAMMER spacecraft in kinetic impactor mode is not an adequate solution for deflecting Bennu (or similar/more challenging NEOs). This raises the question of: for what size NEO can a single HAMMER in kinetic impactor mode produce an adequate deflection? Understanding the capability of a single kinetic impactor HAMMER is important, because we want a system that is fully capable of robustly achieving the threshold deflection mission with a single spacecraft. That allows us to then deploy a campaign of several such spacecraft for mission robustness through redundancy. By contrast, a deflection mission that depends on the success of several spacecraft is much less reliable.

For the case of Bennu, we find that, with a 10-year launch lead-time and $\beta = 1$, a single HAMMER in kinetic impactor mode can adequately deflect an NEO up to 123.8 m in diameter by ~1.4 Earth radii, or deflect an NEO up to 143.62 m in diameter by ~0.25 Earth radii. Note that both cases assume an asteroid bulk density of 1 g/cm^3 and Bennu's orbit. This is important to keep in mind, because the answer will vary depending on

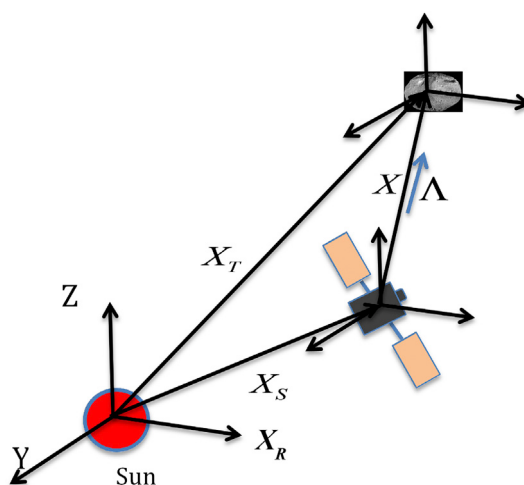


Fig. 13. Asteroid intercept and rendezvous geometry.

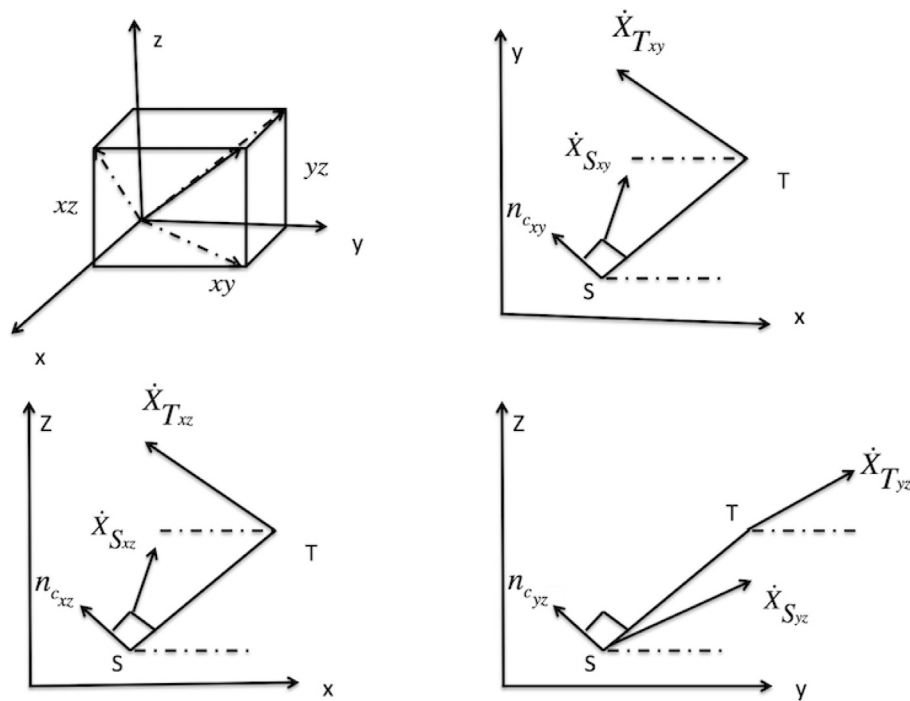


Fig. 14. Projections of Spacecraft Relative state vector onto Three Planes (xy, xz and yz).

NEO orbit, bulk density, launch lead-time, warning time (which, as noted previously, is not the same as launch lead-time, and other factors.

To quantify some of the variability in the size of NEO that can be dealt with via a single HAMMER, we hold the orbit constant at Bennu's orbit, and then vary the asteroid bulk density, β , and launch lead-time. For each combination of those three parameters, we use our algorithms to compute the largest size asteroid that a single HAMMER spacecraft could deflect 1.4 Earth radii from Earth's surface. These results are presented in Table 5.

We observe in the foregoing results that there is an apparent scaling relationship that may be exploited to predict asteroid deflection

performance for a particular mission scenario without the need to execute the trajectory grid calculations. This allows us to predict the total spacecraft mass required to deflect a given asteroid mass by a certain amount, provided that we already know how much spacecraft mass is required to impart that amount of deflection to an asteroid of some other mass. We begin with the equivalency, following from linear momentum conservation, given by

$$\beta_1 = \frac{\bar{m}_1}{M_1 + \bar{m}_1} = \beta_2 \frac{\bar{m}_2}{M_2 + \bar{m}_2} \quad (3)$$

where M_1 is asteroid mass, β_1 is the momentum enhancement parameter

Table 7
The given initial conditions one day prior to Asteroid Intercept.

Body stats	x [km]	y [km]	z [km]	x [km/s]	y [km/s]	z [km/s]
Asteroid-Bennu's Orbit	-35005191.005	133007414.776	14545381.55	-33.091	5.293	5.293
Perturbed spacecraft	35242510.768	132933523.539	14427507.779	-30.345	-30.345	0.776

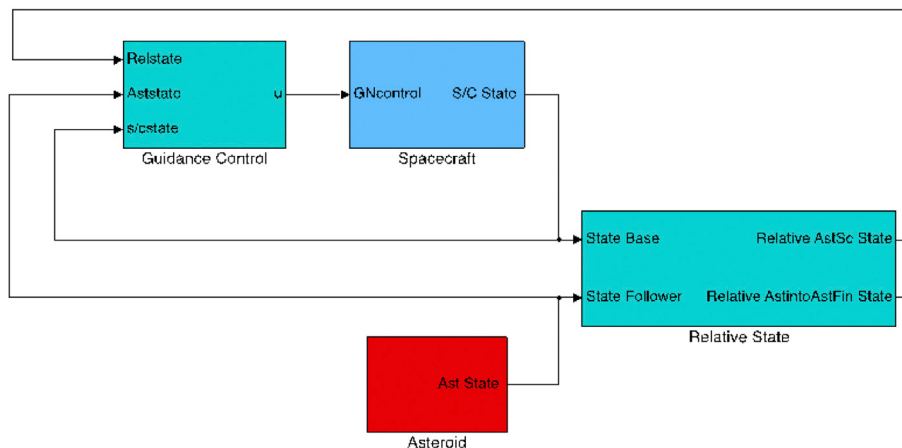


Fig. 15. Schematics of the Asteroid, Spacecraft and guidance controller software implementation.

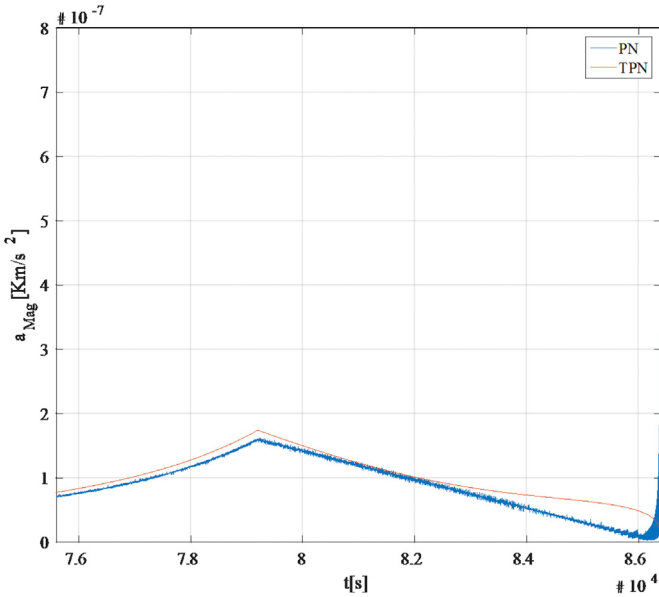


Fig. 16. Acceleration command profile for PN and TPPN controllers.

used in the calculation of the asteroid's deflection, and \bar{m}_1 is the total spacecraft mass used to deflect the asteroid. Those same parameters subscripted "2" correspond to a different case of interest for which we seek to solve for one of the three parameters given the other two. Note that, for a multiple launch scenario, the total spacecraft mass is simply the sum of the masses of the individual spacecraft used to impact the asteroid, given by

$$\bar{m}_1 = \sum_{i=1}^{N_1} m_{1_i} \quad (4)$$

where N_1 is the number of launches and m_{1_i} is the mass of the i th spacecraft. If the mass of each of the N spacecraft is the same, then Eq. (4) reduces to

$$\bar{m}_1 = N_1 m_1 \quad (5)$$

We apply these relationships by manipulating Eq. (3) to yield a scale factor, S_2 , given by

$$S_2 = \left(\left(\frac{\bar{m}_2 \beta_2}{\bar{m}_1 \beta_1 \rho_2 V_{unit_2}} \right) (\rho_1 S_1^3 V_{unit_1} + \bar{m}_1) - \frac{\bar{m}_2}{\rho_2 V_{unit_2}} \right)^{\frac{1}{3}} \quad (6)$$

where $M_1 = \rho_1 V_1 = \rho_1 S_1^3 V_{unit}$, ρ is the asteroid's density, S is the scale factor corresponding to a particular asteroid radius/diameter, and V_{unit} is the volume of the object when the radius is normalized to a maximum value of 1 (unit radius volume). If each of the two asteroids being considered has the same shape, then the unit radius volume will be equal for both bodies.

When the mass of each asteroid is much greater than the total spacecraft mass impacting the asteroid (\bar{m}_1 and \bar{m}_2), and the spacecraft mass per launch is constant, then the scale factor reduces to

$$S_2 \approx \left(\frac{\rho_1 \beta_2 N_2}{\beta_1 \rho_2 N_1} \right)^{\frac{1}{3}} S_1 \quad (7)$$

The scale factors used for Tables 5 and 6 are for the diameters of each object. In addition, the known parameters are variables with the subscript "1," and the input variables are β_2 , N_2 , and ρ_2 .

A similar expression, manipulating Eq. (3) and assuming that each

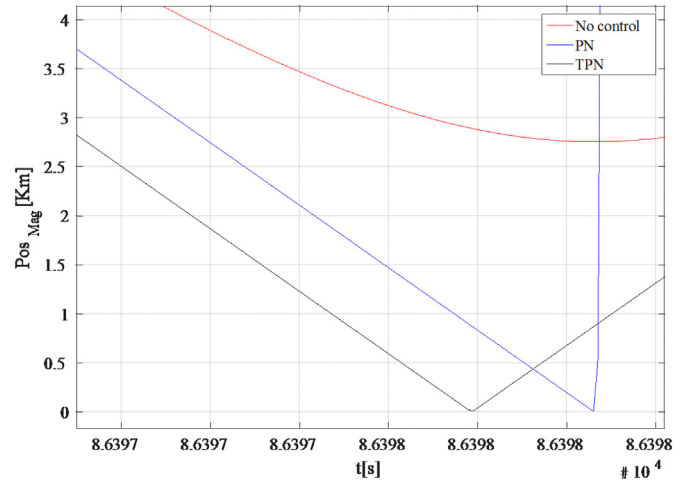


Fig. 17. Relative position magnitude without guidance control, with PN and TPPN controller.

system launch vehicle has the same mass (i.e. $\bar{m} = Nm$), can be found for the number of launch vehicles required

$$N_2 = \frac{M_2}{\frac{\bar{m}_2 \beta_2}{N_1 m_1 \beta_1} M_1 + \left(\frac{\beta_2}{\beta_1} m_1 - m_2 \right)} \quad (8)$$

This equation can be further reduced when the following assumptions are made: $m_1 = m_2 = m$, asteroid is same shape, $M_1 \gg N_1 m$, and $M_2 \gg N_2 m$.

$$N_2 \approx \frac{\rho_2 \beta_2 S_2^3}{\rho_1 \beta_1 S_1^3} N_1 \quad (9)$$

When investigating estimation of launch vehicles across launch vehicle types and deflections, it has been found that the number of launch vehicles can be closely predicted. This is done by taking ratios from other deflections and intercept dates. Note, the deflections in each lead-time must be the same, but each lead-time group can have a different deflection. See Tables 2–4. The relation is as follows

$$N_2(LT_2, LV_2) \approx \frac{N_2(LT_2, LV_2)}{N_1(LT_1, LV_2)} N_1(LT_1, LV_1) \quad (10)$$

Where the LT is the lead-time, LV is launch vehicle type, and N is the number of launch vehicles required as a function of LT and LV. An example to find the number of LVs needed to deflect the asteroid 0.25 RE with a 25 year LT using the data in Tables 2 and 4 is as follows: $N_1(LT_1, LV_1) = 12$ (SLS), $N_1(LT_1, LV_2) = 30$ (Delta IV), and $N_2(LT_2, LV_2) = 10$ (Delta IV). Inputting these values into Eq. (10) yields 4 (SLS), which is the number of Launch vehicles required for deflecting the asteroid about 0.25 RE with a LT of 25 years. However, further investigations must be conducted to explore the reliability of launch vehicle estimation when intercept dates greatly vary in the same lead-time.

4. Preliminary work on terminal guidance

The analysis results discussed previously for asteroid deflection mission design focus on the availability of launch opportunities and associated deflection performance. However, all of those results presume that the spacecraft has sufficient terminal guidance, navigation, and control abilities (sensors, actuators, algorithms, etc) to reliably strike the target NEO when encountering the NEO at a relative speed of several km/s or more. This is a very challenging task, particularly for target NEOs with diameters of several hundred meters or less. Such NEOs are the most likely targets for planetary defense missions, as smaller NEOs are far

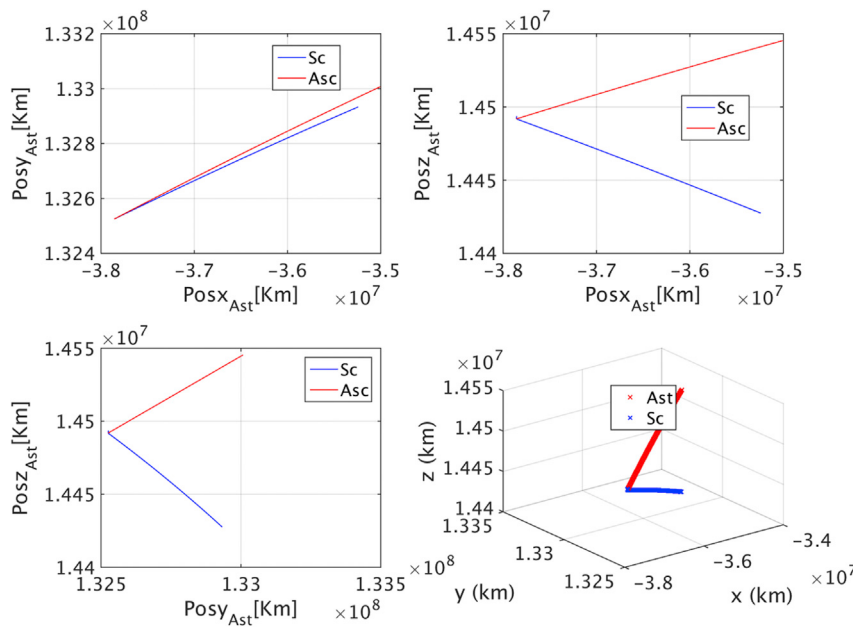


Fig. 18. Position states as viewed in 2D planes and 3D space. Shows relative states convergence for both TPN and PN controllers.

more numerous than their larger counterparts, and so we are more likely to be confronted with a smaller Earth-impacting NEO scenario.

Although the subject of the foregoing mission design analysis, Bennu, is ~ 500 m in diameter, in the following section we will examine terminal guidance performance for the more stressing case of a 50–100 m diameter target NEO. Furthermore, it is likely that ~ 50 m is the smallest diameter NEO we would ever consider deflecting (because smaller NEOs are unlikely to penetrate deeply enough into the atmosphere and/or carry enough energy to be worth the effort/expense of a spacecraft mission deflection). So, it makes sense to design the terminal guidance system such that it can handle the most stressing case because any such terminal guidance would naturally be able to handle the less stressing cases of larger NEOs, to include NEOs of Bennu size and larger.

In this section we present current results for an ongoing investigation into terminal guidance algorithm design for intercept of NEOs, with the eventual goal of being able to robustly intercept NEOs as small as ~ 50 m in diameter. These results are preliminary in the sense that the design efforts are ongoing and will be refined in our next case studies.

Hypervelocity (generally, >5 km/s) NEO intercept speeds in

combination with small NEO diameters are critical challenges for a successful planetary defense mission involving NEO intercept, as the NEO will not fill the Field of View (FOV) of the terminal guidance sensor until a few seconds before spacecraft impact. The investigation needs to consider the error sources modeled in the navigation simulation, such as spacecraft initial state uncertainties in position and in velocity, 3-axis spacecraft attitude uncertainty, and random centroid pixel noise with bias.

Herein we present three selected spacecraft guidance algorithms for NEO intercept and rendezvous missions [9,10]. The selected algorithms are classical Proportional Navigation (PN) [11] based guidance that uses a first order difference to compute the derivatives [12], Three Plane Proportional Navigation (TPPN) [13] and the Kinematic Impulse (KI) [9, 12,14]. These algorithms are implemented in software and tested using a specific mission scenario example.

4.1. Terminal guidance, navigation and control subsystem

The NEO intercept mission will end with a terminal intercept

Table 8

Case study 1 summary of mission objectives and mission goals/requirements.

Mission Objectives	Mission Goals/Requirements	Comments
Track, Intercept, and Divert, using a KI as option if viable	Deliver as much mass as possible, maximize deflection; closing velocity up to 10 km/s	May challenge spacecraft control authority
Utilize largest commercially available US launch vehicle	Absolute navigation accuracy ± 5 km	
Consider use of depleted uranium ($\rho = 19.1$ g/cm 3) in order to use full capability of the Delta IV Heavy class launch vehicle (~ 8870 kg payload)	Transition to relative nav ~ 1 -1 day	Overall response time due to round trip time delay becomes a limiting factor
Maintain Operational readiness	Maintain guidance until impact, with max telemetry	Overall mission duration and mission lead-time become limiting factors
Robust and resilient architecture	Provide diagnostic telemetry for off-nominal events	
Class A+ reliability for deployed system	Fail operational during mission critical phases	"Overall, mitigation" FOM (figure of merit) needs consideration
Ready accommodation of KI or NED payload	Fail safe during non-critical phases	
Max Range: 2.4 au from Earth; 1.4 au from Sun		

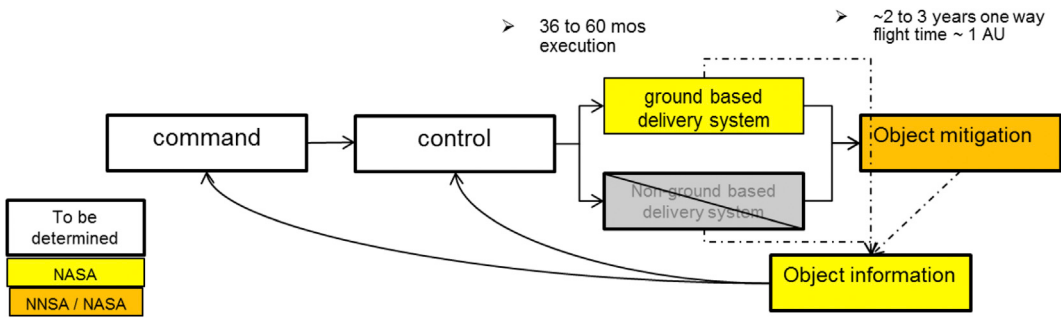


Fig. 19. PHA/PHO mitigation control loop concept.

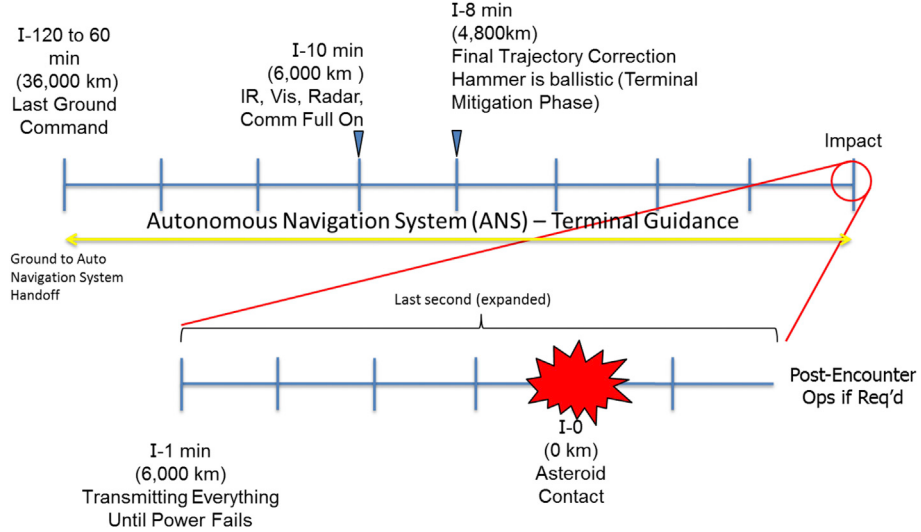


Fig. 20. Case 1 study mission and expanded impact timelines.

guidance phase that requires execution of guided trajectory correction maneuvers to compensate for errors in our knowledge of the target NEO's orbit. This phase starts after the on-board sensors acquire the target NEO states. For example, for a small target NEO (e.g., 50–100 m) the terminal phase might start 2 h prior to intercept, but for a larger NEO or comet it might start earlier. This is because larger objects will tend to have bright apparent magnitudes (assuming comparable surface reflectivities, approach phase angles, and terminal guidance sensor sensitivities, etc), and, therefore, be visible to the spacecraft sensors at greater distances.

The Terminal Guidance, Navigation, and Control (GNC) subsystem is one of the key subsystems of the Asteroid intercept and rendezvous mission. Fig. 12 presents a block diagram for the Asteroid Intercept GNC concept that is modeled in simulation to emulate the NEO intercept mission scenarios. GNC must be done autonomously based on on-board measurements of the NEO states as commanding from Earth via a communications link would otherwise introduce a time-delay that will not be tolerated for hypervelocity NEO intercept missions.

In order to implement the GNC concepts, first the dynamics simulator of the NEO and spacecraft is developed and implemented into software. The GNC is presented in the next section. Fig. 13 gives a graphical representation of the vectors related to the NEO and spacecraft with respect to the sun.

The target NEO is modeled as a point mass in standard heliocentric Keplerian Orbit, as follows:

$$\dot{\mathbf{x}}_T = \frac{d}{dt} \mathbf{x}_T \quad (11)$$

$$\ddot{\mathbf{x}}_T = \mathbf{g}_T \quad (12)$$

$$\mathbf{g}_T = -\frac{\mu_{\odot} \mathbf{x}_T(t)}{\|\mathbf{x}_T(t)\|_2^3} \quad (13)$$

where \mathbf{x}_T is the position vector of NEO with respect to the sun frame, μ_{\odot} is the solar gravitational parameter, and \mathbf{g}_T is the gravitational acceleration due to the sun. Similarly, the dynamics of the spacecraft is derived as:

$$\dot{\mathbf{x}}_S = \frac{d}{dt} \mathbf{x}_S \quad (14)$$

$$\ddot{\mathbf{x}}_S = \mathbf{g}_S \quad (15)$$

$$\mathbf{g}_S = -\frac{\mu_{\odot} \mathbf{x}_S(t)}{\|\mathbf{x}_S(t)\|_2^3} + \mathbf{u}(t) \quad (16)$$

where \mathbf{x}_S is the position vectors of the spacecraft with respect to the sun frame, \mathbf{g}_S is the gravitational acceleration acting on the spacecraft due to the sun, and \mathbf{u} is the control acceleration provided by the spacecraft thrusters. Other disturbing accelerations are neglected due to the assumption of a small NEO [9].

The relative position of the spacecraft with respect to the target NEO is computed as:

$$\mathbf{x}_R = \mathbf{x}_S - \mathbf{x}_T \quad (17)$$

$$\dot{\mathbf{x}}_R = \frac{d}{dt} \mathbf{x}_S - \frac{d}{dt} \mathbf{x}_T \quad (18)$$

Case 1 assumptions (drivers):

- Time of Flight: 740 days
- Intercept Date: July 11, 2113
- Target relative velocity at intercept: 4.48 km/s; concept goal ~10 km/s upper bound, target area goal 100 m dia
- Approach phase angle at intercept: 90.35°
- Maximum Distance from Earth: 1.6 AU
- Maximum Distance from Sun: 1.06 AU
- Total Mission ΔV: 99.2 m/s

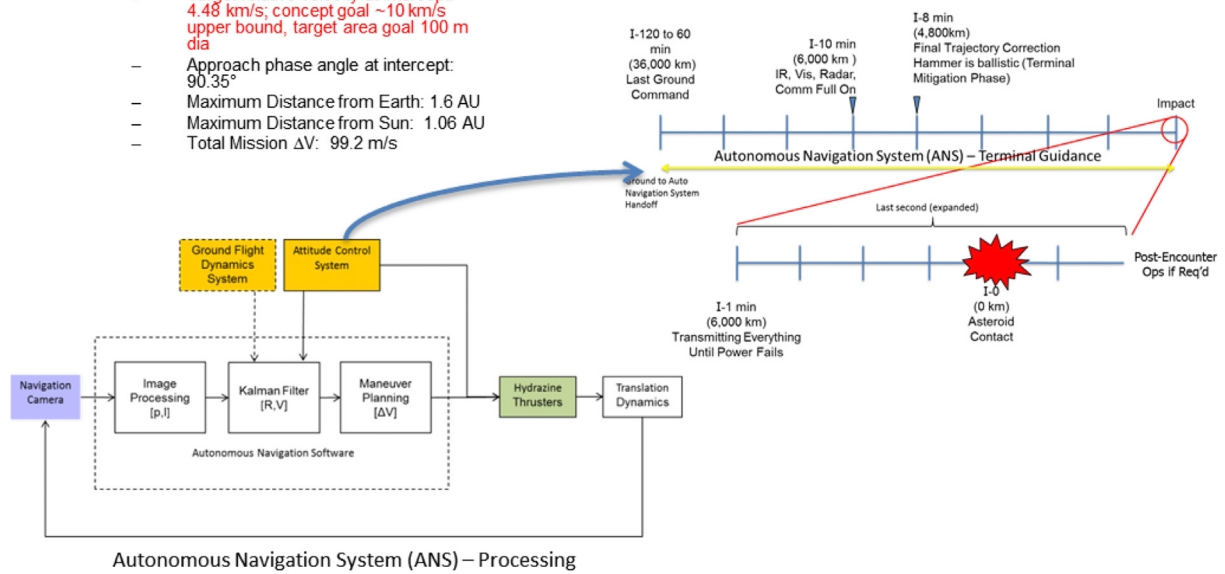


Fig. 21. Autonomous navigation processing subsystem.

$$\ddot{\mathbf{x}}_R = \mathbf{g}_S - \mathbf{g}_T \quad (19)$$

4.2. Spacecraft intercept guidance controllers

Investigation of terminal-phase guidance laws for different mission scenarios is necessary due to different mission requirements and spacecraft capabilities as well as the target NEO parameters. This section reviews three guidance controllers, which are proportional navigation (PN) guidance, Three-plane proportional navigation (TPPN) and kinematic impulse (KI).

4.2.1. Proportional navigation (PN)

The PN guidance law commands acceleration, perpendicular to the instantaneous spacecraft-NEO line-of-sight. The acceleration commands are proportional to the line-of-sight rate and closing velocity. The guidance law can be stated as [11]:

$$\mathbf{u} = nv_c \dot{\lambda} \quad (20)$$

where \mathbf{u} is the control acceleration command, n is a unitless effective navigation gain (usually in the range of 3–5), v_c is the spacecraft-NEO closing velocity, and $\dot{\lambda}$ is the line-of-sight rate.

The closing velocity, time to go, and the line-of-sight rate is computed as follow:

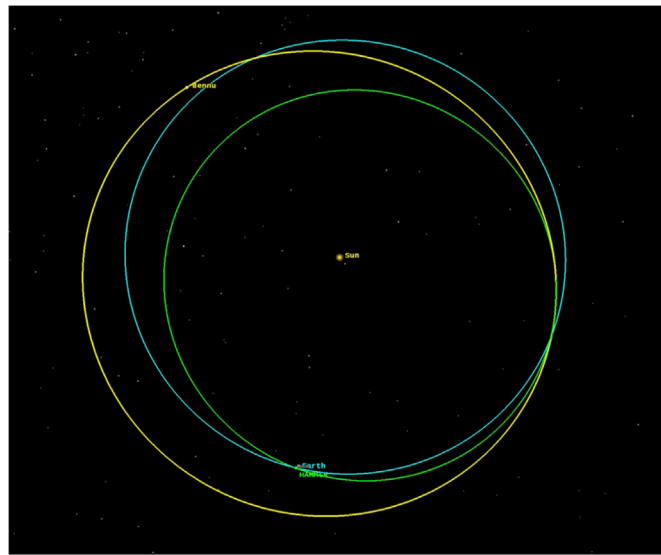


Fig. 22. Heliocentric Trajectory for the Earth Departure Phase. Earth orbit shown in blue, Bennu orbit in yellow, and HAMMER spacecraft orbit in green. (For interpretation of the references to colour in this figure legend, the reader is referred to the web version of this article.)

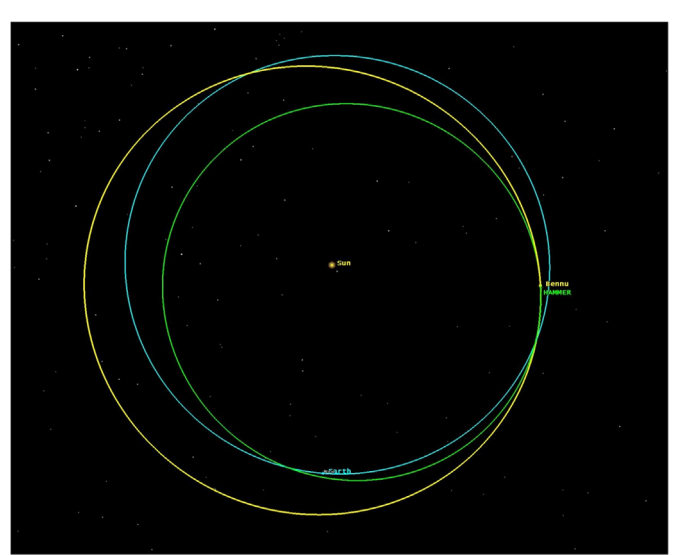


Fig. 23. Heliocentric Trajectory for the Arrival Phase at 10195 Bennu. Earth orbit shown in blue, Bennu orbit in yellow, and HAMMER spacecraft orbit in green. (For interpretation of the references to colour in this figure legend, the reader is referred to the web version of this article.)

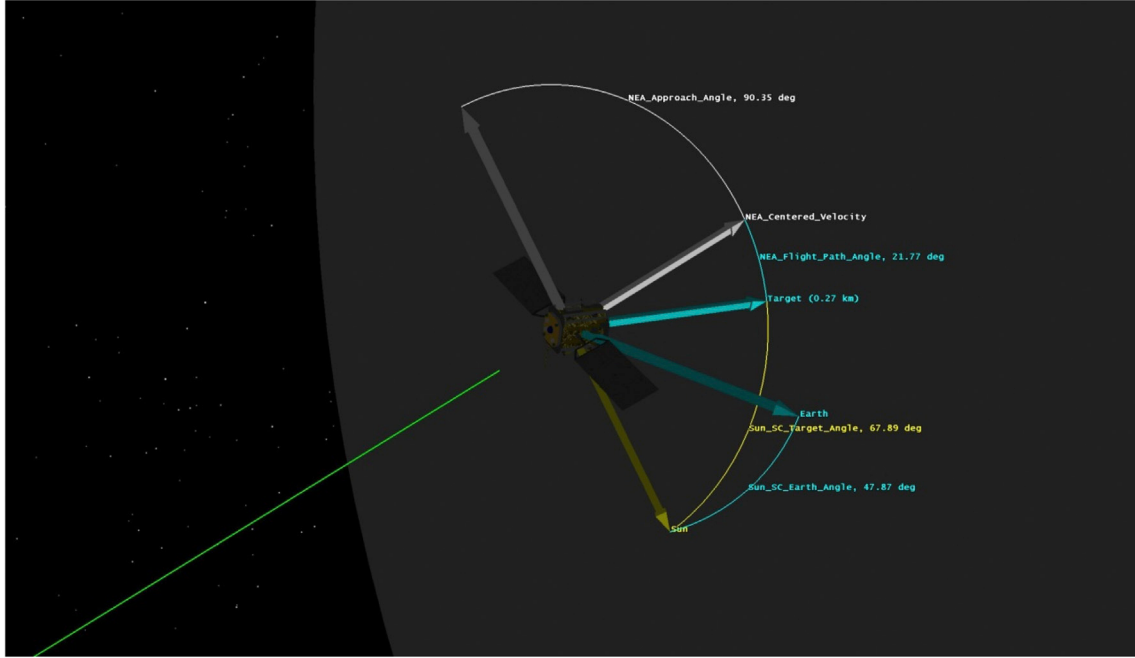


Fig. 24. Final Approach Angles, Geometry and Spacecraft Orientation with the Target. Note that in this figure, the NEO is only in partial view with respect to the spacecraft in the foreground.

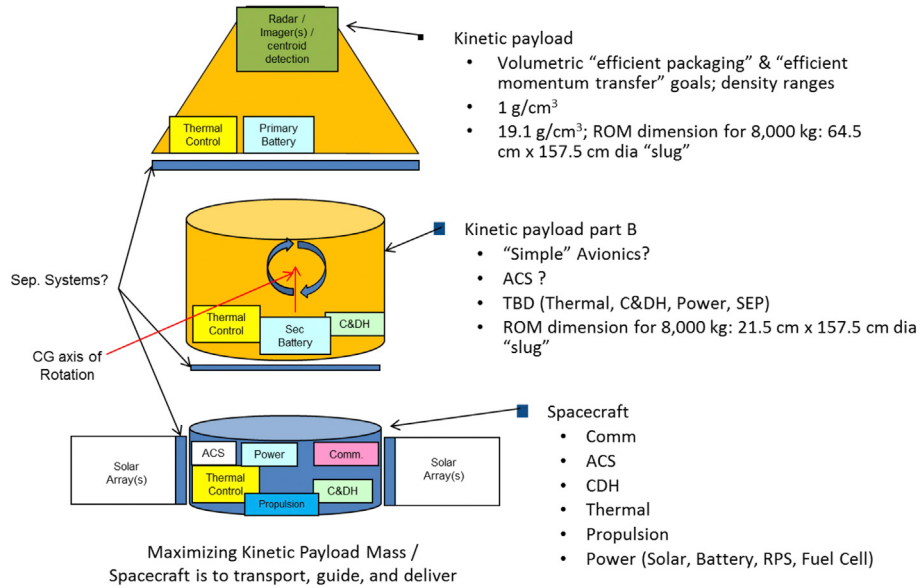


Fig. 25. Modular Decomposition of HAMMER functions.

$$v_c = -\dot{\mathbf{x}}_R \cdot \lambda \quad (21)$$

$$\Delta t = \frac{\|\mathbf{x}_R\|_2}{v_c} \quad (22)$$

$$\lambda(t) = -\frac{\mathbf{x}_R(t)}{\|\mathbf{x}_R(t)\|_2} \quad (23)$$

$$\dot{\lambda} = \frac{d\lambda}{dt} \approx \frac{\lambda(t) - \lambda(t - \delta t)}{\delta t} \quad (24)$$

4.2.2. Three Plane Proportional Navigation (TPPN)

The three-plane approach for 3D true proportional navigation was

designed for a missile to target intercept [13], which is adapted for spacecraft to NEO intercept in this report. The TPPN method projects the spacecraft-NEO relative motion onto the xy , xz , and yz planes and then solves the problem in each plane independently for two-dimensional true proportional navigation. This produces a 3D solution by combining these 2D solutions. Fig. 14 shows the three-dimensional engagement space projected onto three perpendicular planes: xy , xz and yz . From Fig. 14, the 3D solution are derived by combining the components of 2D solutions and equations. The line of sight (LOS) angles:

$$\lambda_{xy} = \tan^{-1} \left(\frac{y_R}{x_R} \right) \quad (25)$$

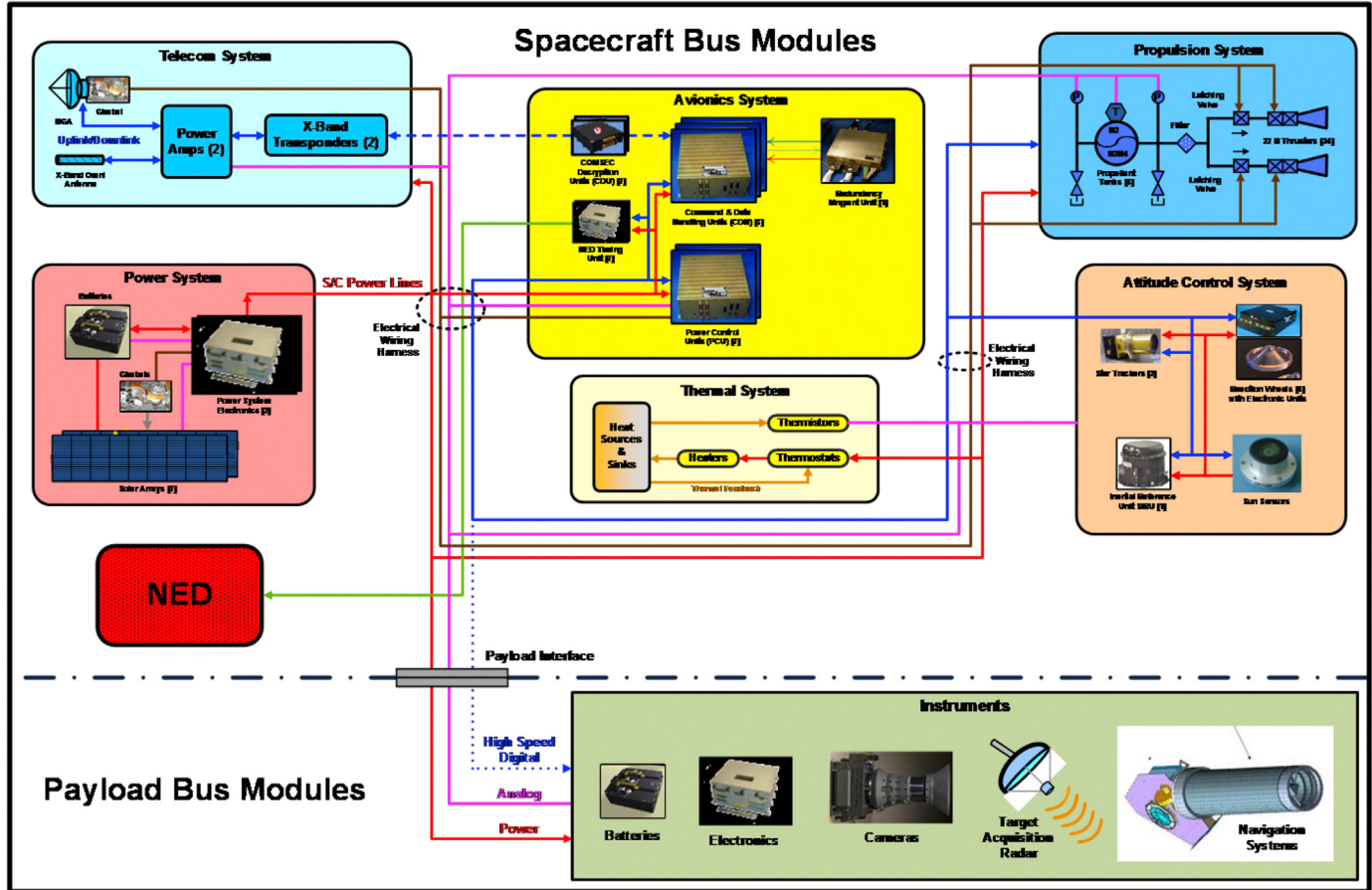


Fig. 26. Spacecraft subsystems functional block diagram as allocated for the case 1 study.

$$\lambda_{xz} = \tan^{-1} \left(\frac{z_R}{x_R} \right)$$

(26) + where x_R , y_R , and z_R are the position components of the relative state vector, \mathbf{x}_R . Line of sight rates for each plane are found to be:

$$\lambda_{yz} = \tan^{-1} \left(\frac{z_R}{y_R} \right)$$

$$\dot{\lambda}_{xy} = \frac{x_R \dot{y}_R - y_R \dot{x}_R}{x_R^2 + y_R^2}$$

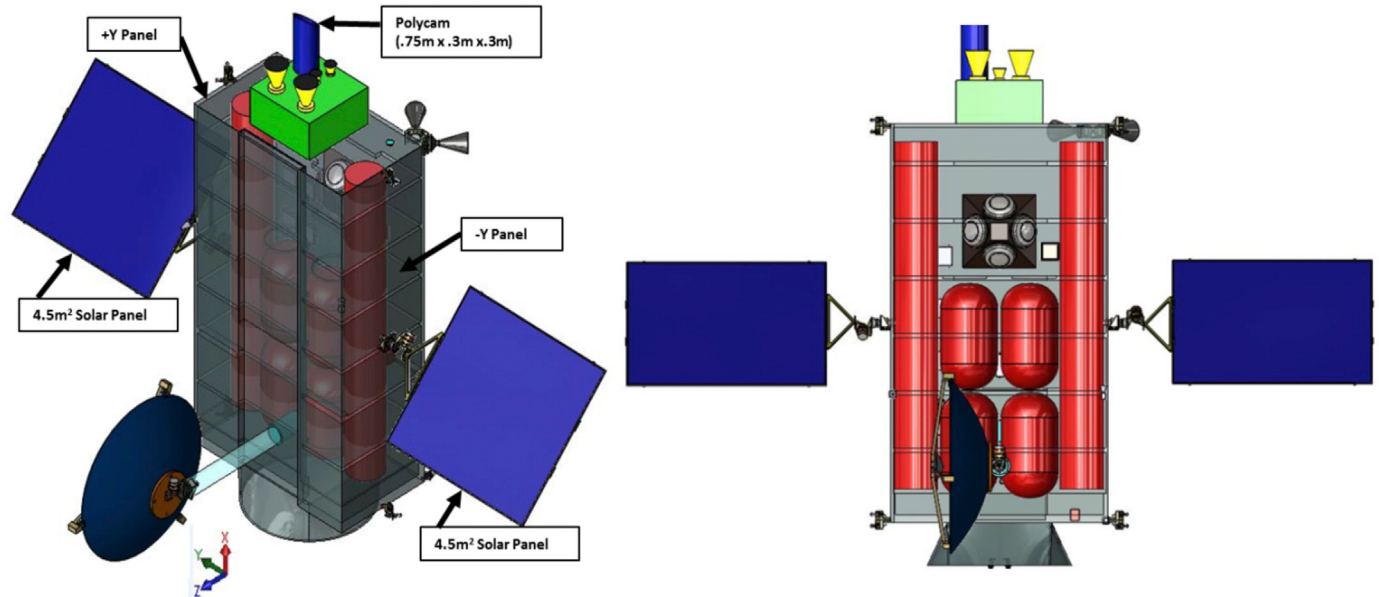


Fig. 27. Case study 1 notional point of departure spacecraft.

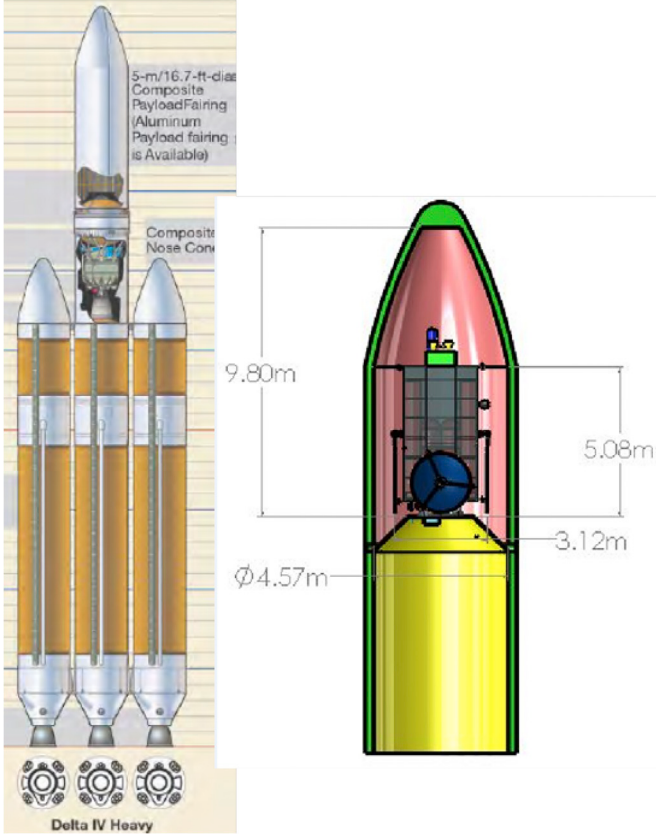


Fig. 28. Case study 1 HAMMER within the Delta-IV heavy fairing.

$$\lambda_{xz} = \frac{x_R \dot{x}_R - z_R \dot{z}_R}{x_R^2 + z_R^2} \quad (29)$$

$$\lambda_{yz} = \frac{y_R \dot{z}_R - z_R \dot{y}_R}{y_R^2 + z_R^2} \quad (30)$$

where \dot{x}_R , \dot{y}_R , and \dot{z}_R are the velocity components of the relative state vector, \mathbf{x}_R . The closing velocities for each plane are computed as:

$$v_{cxy} = -\frac{x_R \dot{x}_R + y_R \dot{y}_R}{\sqrt{x_R^2 + y_R^2}} \quad (31)$$

$$v_{cxz} = -\frac{x_R \dot{x}_R + z_R \dot{z}_R}{\sqrt{x_R^2 + z_R^2}} \quad (32)$$

$$v_{cyz} = -\frac{y_R \dot{y}_R + z_R \dot{z}_R}{\sqrt{y_R^2 + z_R^2}} \quad (33)$$

Hence, the acceleration commands for each plane are derived as follow:

$$n_{cxy} = m v_{cxy} \lambda_{xy} \quad (34)$$

$$n_{cxz} = m v_{cxz} \lambda_{xz} \quad (35)$$

$$n_{cyz} = m v_{cyz} \lambda_{yz} \quad (36)$$

where m is the effective navigation ratio and is bounded by:

$$3 \frac{\|\dot{\mathbf{x}}_S\|_2 - \|\dot{\mathbf{x}}_T\|_2}{\|\dot{\mathbf{x}}_S\|_2} < m < 3 \frac{\|\dot{\mathbf{x}}_S\|_2 + \|\dot{\mathbf{x}}_T\|_2}{\|\dot{\mathbf{x}}_S\|_2} \quad (37)$$

Table 9

Case Study 1 Total Mass Summary (C_3 of $\sim 10 \text{ km}^2/\text{s}^2$) Unused LV Throw Mass 7 kg.

Hammer MASS Summary			
Payload Mass			
Hammer Payload Dry Mass	CBE	Cont.	MEV
Hammer Payload (Inert)	1000.0 kg	0%	1000.0 kg
Hammer Payload (Non-Inert)	1000.0 kg	0%	1000.0 kg
Hammer Payload (Balance)	600.0 kg	0%	600.0 kg
Polycam	9.0 kg	30%	11.7 kg
Radar	100.0 kg	30%	130.0 kg
Optical Camera	5.0 kg	30%	6.5 kg
Total Payload Mass	2/14.0 kg	30%	2748.2 kg
Bus Dry Mass			
Hammer Spacecraft Bus Dry Mass	CBE	Cont.	MEV
Mechanical	3460.2 kg	30%	4498.3 kg
Thermal	36.1 kg	30%	46.9 kg
Attitude Control	57.5 kg	30%	74.8 kg
Propulsion	142.2 kg	30%	184.9 kg
Power	224.0 kg	30%	291.2 kg
Avionics (C&DH)	91.2 kg	30%	118.6 kg
Communications	97.1 kg	30%	126.2 kg
Spacecraft Bus Dry Mass Total	4108.3 kg	30%	5340.8 kg
Observatory Mass			
Hammer Observatory Mass	CBE	Cont.	MEV
Payload Total	2714.0 kg	0%	2748.2 kg
Spacecraft Bus Dry Moss	4108.3 kg	30%	5340.8 kg
Observatory Dry Mass	6822.3 kg	19%	8089.0 kg
Propellant + Gas	774.0 kg	0%	774.0 kg
Observatory Launch Mass	75% . 3 kg		8863.0 kg
Launch Vehicle Evaluation			
LV Throw Mass Margin ^a (Dry Mass) %			0%
Launch Vehicle Capability [Delta IV Heavy]			8870 kg
LV Throw Mass Margin ^a			7 kg

Note: 30% contingency on S/C Bus. Includes redundancy for Class A mission.

Key: CBE: Current Best Estimate, Cont.: Contingency, MEV: Maximum Expected Value.

Notes:

^a MDL Margin Calculation, as weighted against LV capability versus launch mass.

The spacecraft guidance command for each axis can be computed by combining two commands that share the same axis. Thus, the components of acceleration command in each axis is derived as follow:

$$\ddot{x}_S = -n_{cxy} \sin(\lambda_{xy}) - n_{cxz} \sin(\lambda_{xz}) \quad (38)$$

$$\ddot{y}_S = n_{cxy} \cos(\lambda_{xy}) - n_{cyz} \sin(\lambda_{yz}) \quad (39)$$

$$\ddot{z}_S = n_{cxz} \cos(\lambda_{xz}) + n_{cyz} \cos(\lambda_{yz}) \quad (40)$$

Collecting each component yields the control command calculated by TPPN and is given in the control acceleration vector:

$$\mathbf{u} = \begin{bmatrix} \ddot{x}_S & \ddot{y}_S & \ddot{z}_S \end{bmatrix} \quad (41)$$

4.2.3. Kinematic impulse (KI) controller

KI guidance control method is based on the estimation of the line of sight and takes into account the target's future position, utilizing a predictive guidance control approach. The method depends upon a linearized theory to minimize the cost of on-board computations. Predictive guidance needs on-board measurement to estimate the line-of-sight and its rate and knowledge of the target NEO's orbit. The KI method is now in development phase. The next section presents examples based on the PN and TPPN controllers presented above for NEO Bennu's intercept scenario.

Table 10

Case study 1, launch vehicle options.

Vehicle Vs. C3 of 10 Km ² /Sec ²	Delta IV Heavy (2 Launch Pads, SLC-37 ETR and SLC-6 WTR)	Atlas V 551 ETR and WTR (SLC-41, SLC-3E)	Falcon 9 v 1.1 ETR and WTR (SLC-40, SLC-4E)	Ariane 5 (Linear approx.) (One Launch Pad (Korou) Your Mileage May Vary)
	8870 Kg	5060 Kg	2625 Kg	6700 Kg

4.3. Simulation results

Table 7 lists the orbit states for Bennu and the perturbed spacecraft, one day prior to NEO intercept. This data is used to initialize the dynamics of NEO and spacecraft, which are updated for each sampling time. **Fig. 15** shows the schematics of the software implementation of the dynamics and the guidance controllers. The results presented in this section are based on the given data and the implemented software as shown in the schematics.

The guidance laws, PN and TPPN, presented in Section 3 were simulated using the developed Simulink based software. The spacecraft and NEO mass were assumed to be point masses for standard heliocentric Keplerian orbit. The guidance controllers were applied 2 h before estimated intercept or miss time. The guidance simulator runs with a fixed-step sampling time of 0.5 s with a 4-order Runge-Kutta numerical integration scheme.

Fig. 16 shows the computed required acceleration for the standard PN and TPPN guidance controller for the given initial conditions as presented in **Table 7**. The blue line is the acceleration command computed based on a PN controller and the red line is the acceleration command computed based on a TPPN command.

Fig. 17 presents the relative position magnitude profile with and without guidance control. The red label shows relative position magnitude without guidance control. Thus, the initial conditions of the perturbed spacecraft will result in a miss distance of 2.763 km without proper guidance control. The black color line shows a miss distance of around 0.682 km with TPPN guidance control. This miss error can be improved by tuning the effective navigation ratio, m. The blue color shows relative position magnitude with classical PN guidance control. The miss displacement value is around 0.1978 km. The miss distance for

both controllers can be improved by decreasing the fixed sampling time of the spacecraft and NEO state simulator.

Fig. 18 presents the position profiles of the spacecraft and Asteroid Bennu as seen in planes: xy, xz, yz and also in 3D space. The profiles convergence of the spacecraft to the NEO trajectory profile that will cause an intercept of the target NEO Bennu.

5. Overview of the HAMMER (Hypervelocity Asteroid Mitigation Mission for Emergency Response) spacecraft design

As part of the NNSA-NASA collaboration, GSFC's Mission Design Lab (MDL) was engaged to work with a team including members from GSFC, LANL, and LLNL. The goal of this activity was to produce a spacecraft concept capable of intercepting an NEO, functioning as either a Kinetic Impactor (KI) or a Nuclear Energy Device (NED) delivery system. The vehicle was to be modular with separable allocations of the payload allowing change out from a pure Kinetic Impactor to carrying a NED or hybrid payload(s). Spacecraft housekeeping and other delivery functions were to be grouped together to allow for simpler payload-to-spacecraft interfaces. To operate as an effective impactor, HAMMER was sized to the largest mass that could be delivered by a Delta IV Heavy launch vehicle to a range of orbits studied below. This work built upon expertise developed in GSFC's MDL during previous studies that involved the design of similar spacecraft for planetary defense purposes [18,19].

This integrated concept formulation team was combined with the NASA/GSFC facility known as the Integrated Design Center (IDC) as part of the Mission Design Lab (MDL). The IDC is comprised of three concept formulation and design labs; the Architecture Design Lab (ADL), the Instrument Design Lab (IDL) and the aforementioned MDL. The IDC is a NASA resource utilized to conceptualize and perform tradeoffs for future

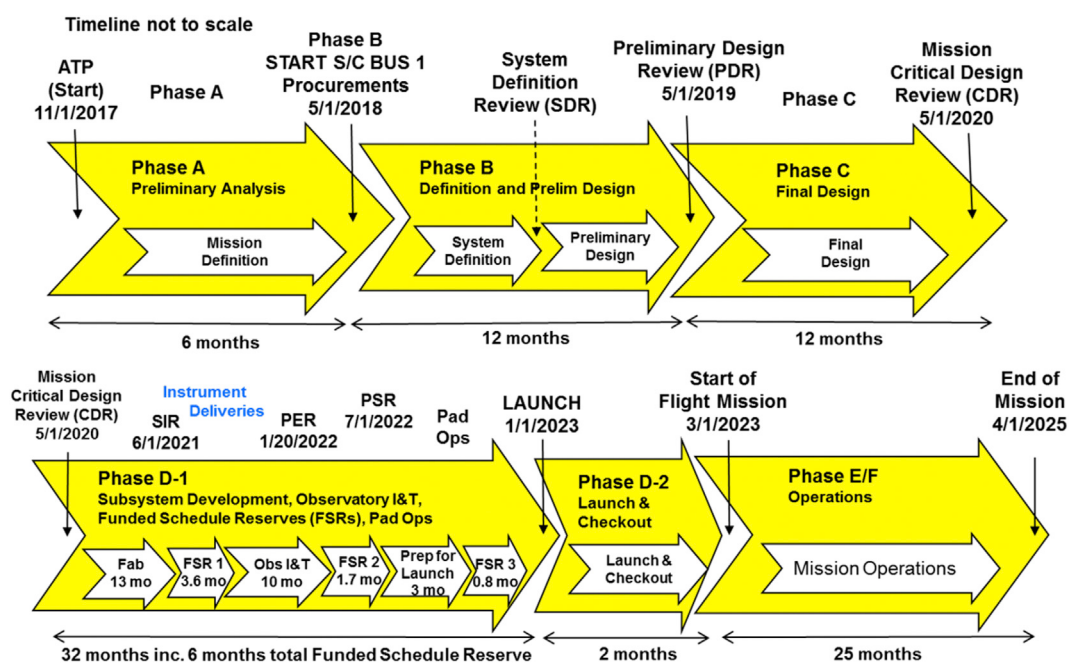


Fig. 29. Case study 1, mitigation mission development and deployment timeline.

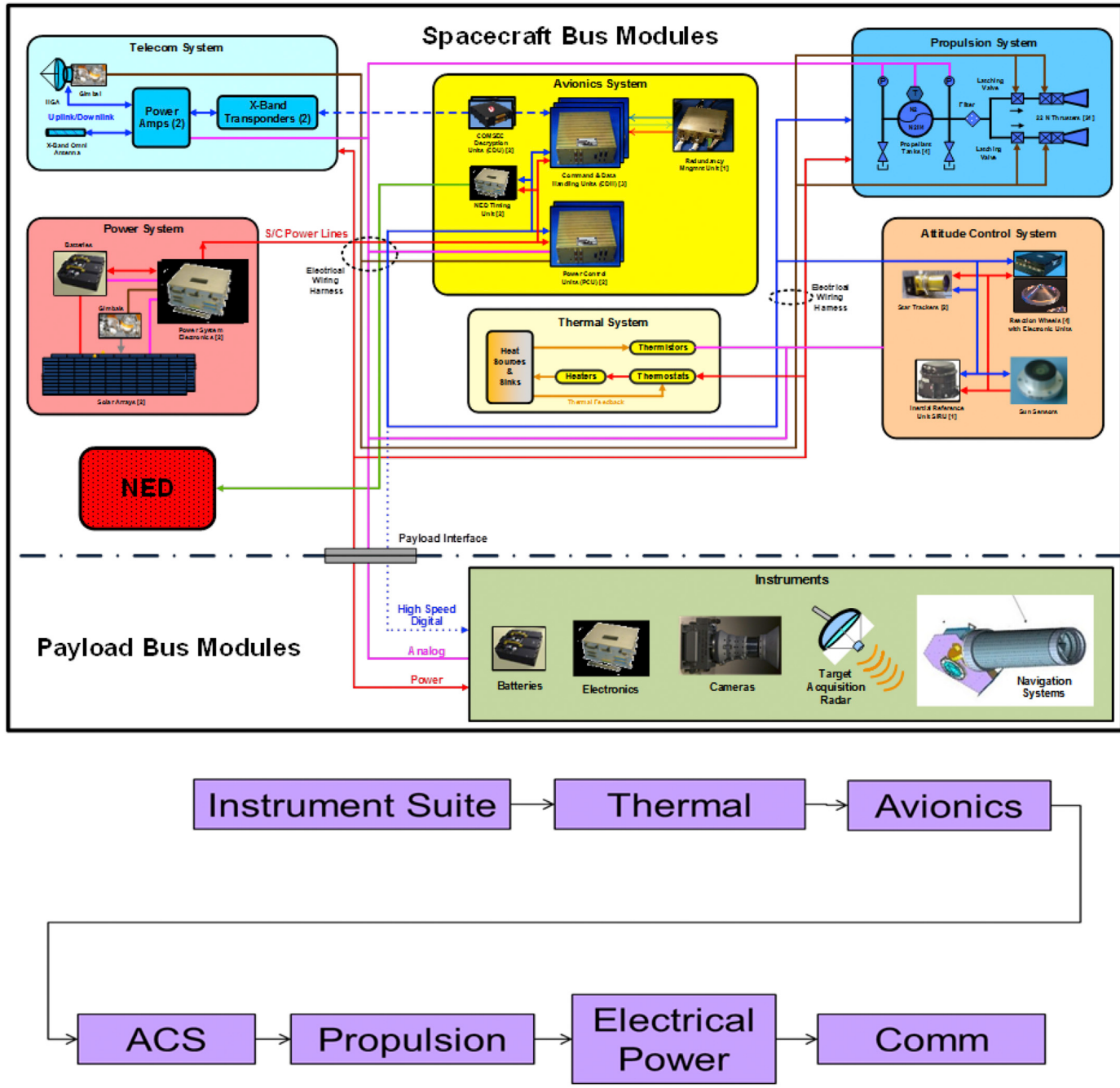


Fig. 30. Preliminary assessment of case 1 study mission reliability.

concepts both for NASA and NASA study partners.

The MDL engaged a team of GSFCs flight hardware discipline engineers to work with GSFC, LANL, and LLNL NEO-related subject matter experts during a one-week intensive concept formulation study in an integrated concurrent engineering environment. This activity produced a detailed concept of a spacecraft to carry out planetary defense mission objectives. While the Bennu scenario was utilized for analysis purposes, the spacecraft concept is intended to be applicable to a broader range of possible hazardous NEA scenarios. The study objective was to formulate a spacecraft concept capable of intercepting an NEO, functioning as either a Kinetic Impactor (KI) or a Nuclear Energy Device (NED) delivery system. The assumed target for this study is the Potentially Hazardous [to Earth] Asteroid (PHA) known as 101955 Bennu (1999 RQ₃₆), which is the destination for NASA's OSIRIS-REx NEO sample return mission,

launched in September 2016 [5].

The spacecraft's performance as a KI was modeled in the MDL, with the goal that it also could function as an NED delivery system (with the NED installed in the spacecraft). Accordingly, the spacecraft would be capable of housing the NED and transporting it to the targeted NEO with the goal of little or no changes to the spacecraft. Thus, the resulting higher-level objective for the MDL study was:

A further objective was to develop a concept for a multi-functional spacecraft (operating alone or as part of a campaign including multiple spacecraft), deliverable to a target NEO by a variety of current and planned US launch vehicles or other launch delivery systems.

The spacecraft concept and corresponding mission profile developed during the MDL study was named HAMMER (Hypervelocity Asteroid Mitigation Mission for Emergency Response).

Table 11
Case 1 study spacecraft subsystem reliability including duration and modes.

	Mode	Reliability
ACS	Full Mission	0.9989
Avionics	Cruise (710 Days)	0.9994
Avionics	Final 30 Days	1.0000
Instruments	Cruise (Standby)	0.9919
Instruments	Final 30 Days	0.9966
Power	Full Mission	0.9994
Propulsion	Full Mission	1.0000
Thermal	Full Mission	0.9987
Design Reliability	Full Mission	0.9849
Launch		0.9800
Mission Reliability		0.9652

Table 12
Case 1 study delivery of multiple of payloads improving campaign Reliability.

k of n	Mission Reliability	95% Confidence
1 of 1	0.9652	0.9362
1 of 2	0.9988	0.9959
2 of 2	0.9316	0.8764
1 of 3	1.0000	0.9997
2 of 3	0.9964	0.9883
3 of 3	0.8991	0.8205
1 of 4	1.0000	1.0000
2 of 4	0.9998	0.9990
3 of 4	0.9931	0.9776
4 of 4	0.8678	0.7681
1 of 5	1.0000	1.0000
2 of 5	1.0000	0.9999
3 of 5	0.9996	0.9976
4 of 5	0.9887	0.9642
5 of 5	0.8376	0.7191
1 of 6	1.0000	1.0000
2 of 6	1.0000	1.0000
3 of 6	1.0000	0.9998
4 of 6	0.9992	0.9955
5 of 6	0.9834	0.9486
6 of 6	0.8084	0.6732

6. Concept formulation constraints and drivers

Table 8 provides the key concept formulation objectives and constraints of this mitigation concept. Due to the desire of utilizing dual modular payloads of both Kinetic Energy (KE) and NED, the mission type is a Class A+ reliability level.

Class A missions are extremely critical operational systems where all practical measures are taken to ensure mission success. They have the highest cost, are of high complexity, and the longest mission life with tight launch constraints. Contract types for these systems are typically

cost plus because of the substantial development risk and resultant oversight activities. These missions are achieved by strict implementation of mission assurance processes devised through proven best practices to achieve mission success over the desired life of the system. All practical measures, to include full incorporation of all specifications/standards contract requirements with little to no tailoring, are taken to achieve mission success for such missions. Class A missions are long life, (nominally greater than 5 years) and represent large national investments for critical applications. NASA Class A missions are represented by flagship missions such as the Hubble Space Telescope, Cassini, and the Jupiter Icy Moon Orbiter (JIMO). NSS Class A missions include the Global Positioning System satellite and military communication satellite systems to include Milstar.

Additionally, the selection of the largest commercially available launch vehicle was included as part of the mission objectives.

7. Top level mitigation functions (post detection)

The major functional elements required for the timely mitigation of PHA/PHO employs a feedback loop control system. Once the object has been detected on a hazardous trajectory, actionable object information will be needed both in sufficient detail and in a timely manner in order for a control system to affect the appropriate mitigation action(s). This control system will utilize the necessary in place segments previously depicted as part of the NEO Mitigation Architecture, including a ground segment, launch segment, space segment, and communications segment. For simplification purposes only the key segments are depicted in Fig. 19. There are a number of characteristics which become drivers for this particular control loop: a) the total round trip delay/propagation time of the communications segment (ranging from 1 to possible 3 au); b) the availability (including any delays such as the quantity and availability) of the ground-based delivery system; c) the end-to-end control loop processing time (or loop response time). This system is likely to include potential manufacturing, launch vehicles, launch processing, space crafts, mitigation payloads (to be paired with space crafts), spacecraft command and communications systems, payload command and communications systems, as well as PHA/PHO detection, tracking, navigation and guidance functions. As shown, all of these functions and elements will need to work in coordination with each other in a timely, reliable, and robust manner.

8. Mission timeline

The reference timeline, see Fig. 20, is a launch on January 1st, 2023, with a 1 week on orbit check-out and an expected cruise phase of 740 days. The mitigation/encounter or impact phase commences roughly one day before the January 10th, 2025 impact (I). Autonomous operations begin at that point. Target acquisition engages at around 9000 km from the encounter point with on-board targeting acquisition strategies such as infrared or mass centroid detection. At I-1 hour (around 36,000 km) commit target processing and on-board optical imaging commences; at I-10 min (approximately 6000 km from engagement) the spacecraft's

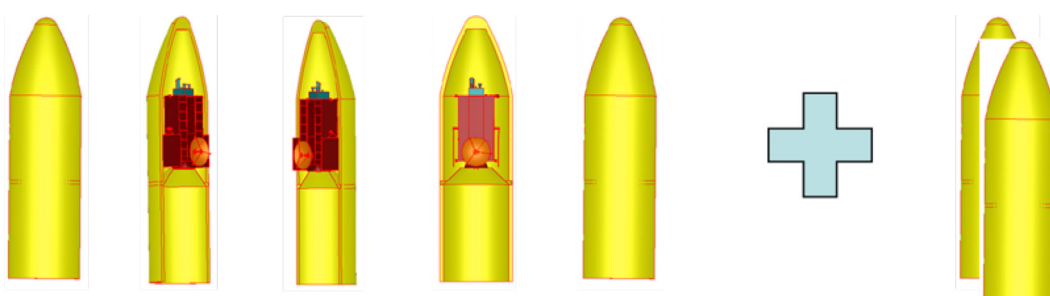
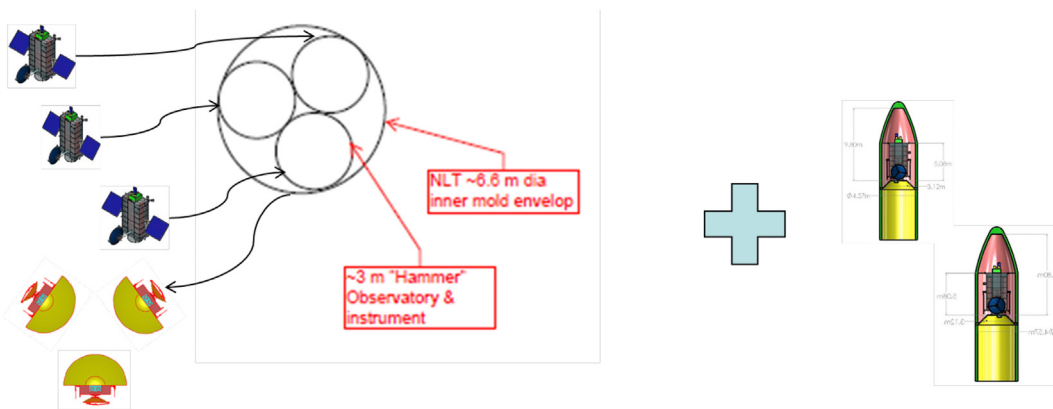


Fig. 31. Multiple launchers.



- What if the “transportation segment” could effectively deliver a set of at least ~5 “observatories” to the PHA of interest and only 1 of the 5 is needed for “mission success?”
- What are ways to accomplish this?
 - What if these 5 HAMMERs could be grouped into a 3 - 1 - 1 delivery system?
 - One 30 mT TBD launch vehicle plus to TBD ELVs?
 - This might be done with 3 launch site + facilities?
 - Candidate for further Brainstorming

Fig. 32. Concept of packaging 3 hammers into a single larger launch vehicle shroud.

velocity relative to the NEO is approximately 4.48 km/s (the formulation concept upper bound goal for NEO relative velocity was established at 10 km/s).

9. Autonomous navigation system

Prior to the terminal navigation timeline phase, the autonomous navigation system (ANS) is in update mode with ground segment systems. It is then corrected and refreshed with information to allow autonomous navigation to take place on-board within spacecraft avionics. This function guides and navigates the spacecraft in the final terminal impact sequence towards the NEO. Fig. 20 shows the closed-loop functional block diagram of this ANS process.

Fig. 21 depicts the ANS subsystem of the terminal approach phase beginning at impact I-2 hours (I-120 min). It depicts the linear covariance analysis, the Monte Carlo error analysis, and utilizes a sequential Kalman filter with observations derived from the NEO centroid location sensor. It solves for the initial position and velocity of the spacecraft with respect to the target NEO.

10. Orbital physics

The next three figures (Figs. 22–24) depict the heliocentric orbit trajectories for the departure, arrival, and final encounter terminal phases. These trajectories determine the environment within which the spacecraft and payload must operate during the launch, transit, and terminal mitigation encounter phases with the NEO.

The above three figures were all simulated using the orbit determination toolbox (ODTBX) software analysis which is an advanced Navigation and Mission simulation and analysis tool used for concept exploration, early concept formulation and/or rapid design center formulation environments. This tool was developed by the Navigation and Mission design Branch at the NASA GSFC.

11. Functional concept

As part of the formulation strategy a functional concept diagram was utilized. This functional block diagram (Fig. 25) was design-approach agnostic. Salient Top level functions of HAMMER are depicted in this figure. The major elements were used as concept building blocks. Multiple or modular kinetic or NED payloads along with partitioning

strategies were conveyed to the concept development team. The separation and simplification of payload to spacecraft interfaces were depicted. This allowed for the partitioning of functions and the trading of these functions between the various elements of payload blocks and spacecraft subsystems.

The top portion contains the kinetic payload which is in the conical section. The center cylindrical section contains simpler/traditional spacecraft avionics such as Attitude Control System (ACS), thermal control system, Command and Data Handling (C&DH), secondary power, separation system and perhaps 8000 kg of another mass slug. The bottom section contains more traditional spacecraft functions such as communications, ACS, C&DH, thermal, propulsion, solar arrays, and power.

The goal was to achieve modular, separable, loosely coupled functional allocations of the payload and spacecraft precision delivery functions. Additionally, the two-part payload concept would allow for change out of one of these as possible NED or hybrid combination payload(s). It is noted that a number of functions are shown in each section. This is to depict both the function(s) potentially needed within each section as well as denoting future allocation trade-offs such as performance or redundancy needs. Spacecraft housekeeping and other delivery functions were to be grouped together to allow for both simpler payload to spacecraft interfaces and to facilitate partitioning of functions within HAMMER, as well as inter-organizational/inter-agency roles and responsibilities. It is anticipated that this functional block diagram will remain a work in progress and will continue to evolve and further develop as additional studies are continued and cases/point-of-departure concepts are considered.

11.1. Subsystem functional allocation for case 1

Fig. 26 depicts the current representation for the Case 1 allocation of spacecraft functions and payload functions. Within the spacecraft there is a telecommunications subsystem, an avionics subsystem, propulsion subsystem, power subsystem, thermal subsystem, attitude control system and (not shown) a control and data handling subsystem. On the lower left is the interface to the NED or kinetic energy device. It's a simpler interface to this modular exchangeable payload. It is a concept goal that one-way data and power are the only necessary interfaces for this modular payload. This concept should allow for modular exchange and very late integration of this payload with the spacecraft. Internal to this payload, it is anticipated that the payload would have its own batteries, control

electronics, detection (camera like) function and target acquisition system as well as some internal navigation detection systems.

Fig. 27 depicts the notional spacecraft concept. It is a rectangular structure where the mechanical/structural loads are carried along its length and through the center of the spacecraft with a thrust tube down the center. The potential NEDs are along the sides. This allows deployment of the NEDs, if necessary. The attitude control thrusters are in the corners of the spacecraft along with a propulsion system (+X axis) to allow release of the NEDs. The solar arrays and the single high-gain antenna are fully gimbaled. This is needed in order to maintain power from a distance of up to 1.4 au from the Sun and communicate to Earth at a distance of up to 2.4 au.

Fig. 28 shows the spacecraft in the launch configuration within the Delta-IV Heavy. It occupies only about two-thirds of the volume since the spacecraft mass is concentrated. The overall fairing size of the Delta-IV Heavy is shown to be about 9.8 m in length, about 4.6 m in diameter within the dynamic fairing envelope. The spacecraft is attached to a 3 m fairing adapter. The overall spacecraft length is just over 5 m.

Table 9 shows the mass rack up for the entire spacecraft plus payload (observatory mass is equal to total payload mass plus total spacecraft wet mass). Please note that the payload carries a 0% contingency as it was used to completely maximize the mass of the launched payload to be delivered (Gross Liftoff Weight (GLOW)). Overall, at the concept level there remains just 7 kg of launch vehicle throw mass margin.

11.2. Alternative launch vehicles

Table 10 shows the options available for all other currently available launch vehicles and their launch capabilities for this point of departure mitigation target. Note that all other launch vehicles have significantly less capability of delivering a payload to the mitigation target.

12. Notional space segment development and deployment timeline

Fig. 29 shows a notional mitigation mission development and deployment timeline. Note that it takes over 64 months in order to complete the development, design, and ATLO (Assembly, Test, and Launch Operations) of the mitigation vehicle and an additional 2 months for near-Earth on orbit verification prior to the departure injection burn. Additionally, 25 months of transit time is needed in order to reach the target. In total, this accounts for over 7 years lead-time (89 mos) for an identified PHA target. This kind of timeline would clearly be problematic for a shorter warning situation, and we are motivated to find ways to compress the timeline as much as possible while maintaining sufficient mission reliability. Such timeline compression would likely be costly in terms of funding, personnel, and other industrial resources, but high resource utilization during an emergency situation would probably be acceptable. Research into approaches to accomplish such mission timeline compression is ongoing.

12.1. Mission effectiveness/mission success

Preliminary mission mitigation effectiveness assessments were made for each of the specific subsystems used for the Case 1 study. As derived from the spacecraft system functional block diagram for this case study, each of the subsystems was modeled. See **Fig. 30** for the system spacecraft functional block diagram along with the RSS functional string assessment methodology. Greater details can be provided within the detailed MDL study customer presentation. This is available only to the government study team personnel by special request. **Table 11** provides the subsystem breakdown by mission mode/phase, and the reliability assessment for each of the subsystems.

Table 12 provides a multiple launch mission reliability trending assessment. K of N Mission reliability and confidence factors are depicted in the table. Key assumptions were made for both the kinetic energy/NED

payload device(s) as well as software reliability. Both of these items were assumed to have a reliability factor of 1 for this initial analysis. From this table, one can see that multiple launches can achieve a high factor of confidence in delivering the payload to the PHO/PHA target. This table does not address the devaluation factors needed to account for both the software as well as the kinetic energy/NED devices. Significantly more detailed work will be needed to account for these additional subsystems as well as any future changes resulting from concept refinements and further developments.

What is noted here, however, is that multiple launched missions have a significant effect in improving of the overall mission confidence as denoted by each of the highlighting arrows. By employing multiple payload deliveries, one can achieve architectures or methods significantly mitigating the payload delivery system (spacecraft/launch vehicle aka transportation space segment) as an impacting factor to the overall mission reliability. It is therefore important to consider multiple launch delivery concepts in future case studies or mission level architecture or segment level concept trades.

12.2. Concept of campaign mode

As an extension to the MDL study Case 1 activities, joint interagency team brainstorm activities continued. This included a reference to the previous **Table 12** under the 95% column for the 1 of 5, k of n. Note that a confidence factor of 1 was nominally/notionally achieved however, this involved the launch or delivery of 5 payloads. This scenario includes a multiple launch delivery analysis suggesting 5 payloads plus 2 spares (see **Fig. 31**). It is suggested that this concept may need further investigation or study along with the associated infrastructure assessments and analysis (launch facilities, launch processing operations, launch ops and support, etc.) For this concept, one may include the packaging of multiple payloads into a single launch vehicle thus reducing launch facility processing burden.

This might be accomplished, in concept, within the SLS system (see **Fig. 32**). The SLS system would be augmented by two additional Delta-IV Heavy launch vehicles. A single SLS block 1A might be capable of delivering 30 metric tons to a PHA/PHO target for mitigation (~3 times the capacity of the Delta-IV Heavy). The two Delta-IV Heavy delivery systems would follow shortly thereafter as a mission reliability improvement concept providing both launch vehicle diversity as well as an additional independent payload delivery system. The total of 5 payloads would be delivered to the intended PHA while the goal is that only one of these is needed to achieve mitigation success. It is suggested that further case study be considered for these kinds of options. Note that there are many issues associated with an attempt to launch multiple spacecraft within a relatively short timeframe, as elaborated upon previously in Section 3. As already stated, these issues are important and need to be addressed, but addressing them is beyond the scope of the work presented herein.

13. Conclusion and future plan

While the kinetic impactor is a simple idea, HAMMER begins to show how complex such a vehicle is. While HAMMER was designed to be capable of either an impactor or nuclear mission, the modular structure provided a flexibility that added little to the spacecraft. As discussed in the introduction, delay is the enemy of an impactor mission. Once a decision is made that an object must be deflected, it is estimated that 64 months will be required to build and prepare the vehicle for launch. Depending on the frequency of an acceptable launch window, there may be a delay for that (not shown in **Fig. 29**). Once launched, the mission shown here for a Bennu-like scenario requires another 25 months to reach the target. While future work includes studying effects of including gravity assist flybys, deterministic deep space maneuvers, and low-thrust propulsion, such activities permit reaching more difficult targets, but do not shorten the response time.

With this there is a minimum of 7.4 years required from decision to an impulse delivered on the NEO. For a Bennu-like orbit, if the 10 km/s window is required, there may be additional years to wait for the launch opportunity. Then, after the impulse is delivered, there is the time required for the speed change to integrate sufficiently for a deflection.

The β values of 1 and 2.5 used in [Tables 2 and 4](#), were simply chosen for examples, and scaling equations are provided. In fact, 2.5 is close to the value for a typical Bennu impact velocity near 5 km/s. It could be as high as 3.9 if the delay in waiting for the 10 km/s window is not an issue. Alternatively if the impact point were on a large strong (100 MPa) boulder, β values drop to near 1.2. For an inhomogeneous body, the surface structure of the impact site matters.

Mission success is never 100% and with an impact threat of a magnitude to require a mission, there is a benefit in sending more than 1 vehicle. However, when the body is large, like Bennu, there is the possibility of attempting to deflect with multiple impactors. This certainly costs time in building the vehicles, and severe resource problems if the vehicles are to be launched in a narrow window. Worse, if multiple impacts are required for a successful deflection, the probability of failure is increases as shown in [Table 12](#), requiring more backup vehicles.

With an eye to future work, in studying the mission parameter tradeoffs, the hypervelocity guidance simulator implemented here includes three guidance controllers: PN, TPPN and KI. This example using NEO Bennu demonstrated that the simulator could be used to test the controllers under different scenarios. In this report, the spacecraft initial state is perturbed in order to evaluate the performance of the PN and TPPN controllers. Both controllers improved the miss displacement between the spacecraft and the target NEO Bennu.

The current work is testing the KI controller using the same data set of NEO Bennu and spacecraft initial perturbed state. Future research will consider a hybrid KI and PN controller for the same scenario and compare it with the independent controllers. In addition, we will introduce error sources in the simulator and try the different controller concepts.

Acknowledgment

This research was supported by NASA ROSES grant NNH14ZDA001N-SSO. Also, this research was supported in part by an appointment to the NASA Mission Directorate Research Participation Program. This program is administered by the Oak Ridge Institute for Science and Education through an interagency agreement between the U.S. Department of Energy and NASA. We further acknowledge that some of this work was performed under the auspices of the U.S. Department of Energy

by Lawrence Livermore National Laboratory under Contract DE-AC52-07NA27344.

References

- [1] T.J. Ahrens, A.W. Harris, Deflection and fragmentation of near-Earth asteroids, *Nature* 360 (1992) 429–433.
- [2] S.R. Chesley, D. Farnocchia, M.C. Nolan, D. Vokrouhlický, P.W. Chodas, A. Milani, F. Spoto, L.A.M. Benner, M.W. Busch, J. Emery, E.S. Howell, D. Lauretta, J.-L. Margot, B. Rozitis, P.A. Taylor, Orbit and bulk density of the OSIRIS-REx target asteroid (101955) Bennu, *Icarus* 235 (June 2014) (2013) 5–22.
- [3] D. Izzo, ESA Advanced Concepts Team, Code used available in MGA.M, on <http://www.esa.int/gsp/ACT/inf/op/globopt.htm>. Last retrieved November 2009.
- [4] E.R. Lancaster, R.C. Blanchard, A Unified Form of Lambert's Theorem, NASA technical note TN D-5368, 1969.
- [5] D.S. Lauretta, et al., The OSIRISREx target asteroid (101955) Bennu: constraints on its physical, geological, and dynamical nature from astronomical observations, *Meteorit. Planet. Sci.* 50 (2015) 834–849.
- [6] H.J. Melosh, I.V. Nemchinov, Yu.I. Zetser, in: U. Tom Gehrels (Ed.), *Hazards Due to Comets and Asteroids*, A. Press, 1994, pp. 1111–1132.
- [7] R.H. Gooding, A procedure for the solution of Lambert's orbital boundary-value problem, *Celest. Mech. Astron.* 48 (1990) 145165.
- [8] National Research Council Reports to Congress, *Defending Planet Earth: Near-earth Object Surveys and Hazard Mitigation Strategies*, 2010.
- [9] M. Hawkins, Y. Guo, B. Wie, Spacecraft guidance algorithms for asteroid intercept and rendezvous missions, *Int. J. Aeronaut. Space Sci.* 13 (2) (2012) 154169.
- [10] B.W. Barbee, B. Wie, M. Steiner, K. Getzandanner, Conceptual design of a flight validation mission for a hypervelocity asteroid intercept vehicle, *Acta Astronaut.* 106 (January–February 2015). Pages 139–159, ISSN 0094–5765.
- [11] P. Janus, John, Homing Guidance (A Tutorial Report) AD-756 973, Space and Missile Systems Organization, 10 December 1964.
- [12] J. Lychoft, M. Hawkins, B. Wie, GPU-based optical navigation and terminal guidance simulation of a hypervelocity asteroid intercept vehicle, *AIAA-2013-4966*, in: *AIAA Guidance, Navigation, and Control Conference*, Boston, MA, August 19–22, 2013.
- [13] I. Moran and T. Altilar, Three plane approach for 3D true proportional navigation, *AIAA Guidance, Navigation, and Control Conference*.
- [14] M. Hawkins, A. Pitz, B. Wie and J. Gil-Fernandez, Terminal-phase guidance and control analysis of asteroid interceptors, *AIAA Guidance, Navigation, and Control Conference*.
- [16] G. Vardaxis, B. Wie, Planetary defense mission design using an asteroid mission design software tool (AMiDST), in: *AIAA-2013-4713*, *AIAA Guidance, Navigation, and Control Conference*, Boston, MA, August 19–22, 2013.
- [17] G. Vardaxis, B. Wie, Planetary defense mission applications of heavy-lift launch vehicles, in: *AAS 15-564, AAS/AIAA Astrodynamics Specialist Conference*, Vail, CO, August 9–13, 2015.
- [18] A. Pitz, B. Kaplinger, G. Vardaxis, T. Winkler, B. Wie, Conceptual design of a hypervelocity asteroid intercept vehicle (HAIIV) and its flight validation mission, *Acta Astronaut.* 94 (2014) 4256.
- [19] B. Wie, et al., An Innovative Solution to NASA's NEO Impact Threat Mitigation Grand Challenge and Flight Validation Mission Architecture Development, NIAC Phase II Final Report, NASA Innovative Advanced Concepts Phase II Study, Sept. 2012 Sept. 2014.